JOURNAL OF MADENAT ALELEM COLLEGE

REFEREED SCIENTIFIC JOURNAL Published
by the University College of Madenat al-elem , Iraq , Baghdad , AlKadmyia

Vol:6 No:1 year: 2014 ISSN: 2073-2295

كلية مدينة العلم الجامعة

Madenat Alelem University College

مجلة كلية مدينة العلم

العراق - بغداد - الكاظمية المقدسة

Journal of Madenat Al-elem College
(JMAC)

WWW.JMAUC.ORG

E-mail: Jmac2009m@yahoo.com

P.O,Box (9216) Tel:5238850

WWW.madenatalelem.com

INSTRUCTIONS to AUTHERS

Submitted articles to the Journal of Madinat Al-Elem University College can be published in all fields related to the Academic Departments of the College (Biology, Law, programming Engineering Sciences, and Computer Techniques Engineering).

Written request for publication and signing a consent form to publish must be for articles which have not been published or submitted for publication to other journals. Three copies with CD are needed. Manuscripts should be typed on: A4 white paper, double spaced, written in Times New Roman font size 14. Margins should be 3cm from top, bottom, left and right. The main title should be in: bold Times New Roman font size 14. Author names should be written in the following sequence: first name, middle name, the family name, followed by the names of departments and institutions of work. A footnote accompanies the first page stating the full address of correspondence author.

Articles need to contain the following items:

- Abstract in English and Arabic not more than 300 words.
- Article includes the following items: Introduction, Materials and Methods, Results and Discussion, Conclusion and References.
- References should be numbered in the text according to the sequence appeared in the text and listed in order.
- Tables and figures should be appropriately titled with size not exceed an A4 page.

The editor reserves the right to reject or accept any article submitted.

Publication charges: Each accepted paper is required to pay the publication charge (100,000 Iraqi dinars). The paper has extra pages should pay 5000 Iraqi dinar for each extra printed page.

Contents

Enhance Criminal Investigation by Proposed Fingerprint Recognition System

Soukaena H. Hashem[1] Abeer T. Maolod[1] Anmar A. Mohammad[1]

[1]*Computer Sciences Department, University of Technology, Baghdad/Iraq*

Ph. 00964 7811332431

Abstract

Law enforcement officers and forensic specialists spend hours thinking about how fingerprints solve crimes, and trying to find, collect, record and compare these unique identifiers that can connect a specific person to a specific crime. These individuals understand that a basic human feature that most people take for granted, can be one of the most effective tools in crime solving.

This research exploits our previous work to be applicable in criminal investigation field. The present study aims to solve the advance crime by strength fingerprint's criminal investigation to control the alterations happen intentionally to criminals' fingerprint. That done by suggest strategy introduce an optimal fingerprint image feature's vector to the person and then considers it to be stored in database for future matching. Selecting optimal fingerprint feature's vector strategy deal with considering 10 fingerprints for each criminal person (take the fingerprint in different time and different circumstance of criminal such as finger is dirty, wet, trembling, etc.). Proposal begun with apply a proposed enrollment on all 10 fingerprint for each criminal, the enrollment include the following consequence steps; begin with preprocessing step for each of 10 images including enhancement, then two level of feature extraction (first level to extract arches, whorls, and loops, where second level extract minutiae), after that applying proposed Genetic Algorithm to select optimal fingerprint, master fingerprint, which in our point of view present the most universal image which include more detailed features to recognition. Master fingerprint will be feature's vector which stored in database. Then apply the proposed matching by testing fingerprints with these stored in database.

While, measuring of criminal fingerprint investigation performance by calculating False Reject Rate (FRR)and False Accept Rate (FAR) for the traditional system and the proposed in criminal detection field. The obtained results encourage to publish this work.

Keywords: Crime Analysis, Criminal, fingerprint, minutiae, genetic algorithm, feature extraction, FRR, FAR.

تعزيزالتحقيقات الجنائي بأقترح نظام التعرف على بصمات الأصابع

سكينة حسن هاشم عبير طارق مولود انمار علي محمد
[1]قسم علوم الحاسب ، جامعة التكنولوجيا ،بغداد / العراق

ملخص

ضباط إنفاذ القانون و الأخصائيين في الطب الشرعي يقضون ساعات في التفكير في كيفية حل الجرائم من خلال الاستقصاء عن بصمات المجرمين، ومحاولة إيجاد وجمع و تسجيل و مقارنة هذه المعرفات الفريدة (البصمات) التي تمكن توصيل شخص معين لجريمة محددة . هؤلاء الأفراد يعرفون تماما ان لكل انسان ميزة أساسية، يمكن أن تكون واحدة من أكثر الأدوات فعالية في حل الجريمة.

هذا البحث سوف يعتمد على بحثنا السابق ليكون قابل للتطبيق في مجال التحقيق الجنائي. لذلك ، الهدف هنا للمضي قدما لحل الجريمة من قبل التحقيقات الجنائية للبصمات للسيطرة على التحويرات التي تحدث عمدا إلى بصمة المجرمين. تم القيام بهذا العمل من خلال اقتراح خطة عمل للحصول على مجموعة خصائص بصمة الاصابع الامثل للشخص ومن ثم يتم تخزينها في قاعدة البيانات للمطابقة في المستقبل. اختيار مجموعة الخصائص الأمثل لبصمة الاصابع سيأخذ بنظر الاعتبار 10 بصمات لكل شخص (أخذ بصمات الأصابع الجنائية في أوقات مختلفة و ظروف مختلفة مثل عندما تكون الاصابع قذرة او رطبة او يرتجف ، الخ). تبدأ تطبيق المقترح بالتسجيل لكل بصمات الأصابع الجنائية بحيث لكل مجرم 10 بصمات ، وتشمل تطبيق الخطوات التالية والتي تبدأ مع خطوة المعالجة الاولية لكل من الصور 10 ، ثم المستوى الثاني المتضمن استخراج الميزات (المستوى الأول لاستخراج والأقواس وفلكات المغزل والحلقات والمستوى الثاني استخراج التفصيلات الدقيقة) ، بعد ذلك يتم تطبيق الخوارزميات الجينية المقترحة لتحديد بصمة الاصابع الأمثل ، البصمة الاساسية ، والتي في وجهة نظرنا تقدم الصورة الأكثر عمومية بحيث تشمل ميزات أكثر تفصيلا تقود الى التمييز الادق. وسوف تكون البصمة الاساسية عبارة عن مجموعة خصائص تخزن في قاعدة البيانات. ثم اجراء المطابقة المقترحة من خلال اختبار بصمات المجرمين مع بصماتم الاساسية التي تم تخزينها في قاعدة البيانات.

لقياس مدى نجاح النظام المقترح لتميز بصمة الاصابع للمجرمين يتم حساب معدل الرفض الكاذب (FRR) ، ومعدل القبول الكاذب (FAR) للنظام التقليدي و المقترح في مجال الكشف الجنائي وكانت النتائج مشجعه لنشر هذا العمل.

كلمات البحث: تحليل الجريمة ، مجرمين ، البصمات ، تفصيلات البصمة، الخوارزمية الجينية ، واستخراج الميزة، FAR . ،FRR

1. Introduction

Every person is born with his own unique set of fingerprints. There is no two fingerprints have ever been found to be exactly alike; not on identical twins (although these are extremely similar), not even on a person's own hand. The unique whorls and lines that make up an individual's fingerprints are formed in the fetal stage and remain the same throughout the entire life span. This makes for a unique mark that can positively identify one individual against another, particularly useful when a person of interest already has a recorded set of fingerprints on file with police, military or other government institutions [1].

Fingerprints are made up of a collection of swirling lines. The way these lines form and pattern themselves is what makes each fingerprint unique. Despite the incredible number of different fingerprints, there are only seven different types of lines that make up fingerprints. These lines may start, stop or split at any place within the print. The formations, angles, lengths, heights and widths make billions and billions of different prints. With their unique qualities, it becomes easy to see how fingerprints can help solve crimes. Leaving a fingerprint is like leaving a calling card at the crime scene. There are few different ways fingerprints get left behind by careless crooks. The most common way is from fat or oil that is transferred from the finger to an object like a doorframe or table. Amino acids from the finger may also leave a discernable mark. Fingerprints can also be detected as an impression in a soft substance such as putty. Finally, they can be made by a substance on the finger such as blood or paint. Uncovering fingerprints to help solve a crime can be done in a few ways. Adhering powders to fresh fingerprints will cause the powder to stick to the grease and make the fingerprint visible. Another method is by using a few drops of cyano-acrylate or superglue. When these drops are heated, they vaporized and the smoke attaches to the fingerprint leaving a clear white print. Specialized crime scene laboratory equipment can also find fingerprints, but not all authorities have access to all equipment.

Fingerprints can be saved for further investigation in a number of ways, including: take a photograph of the print, store it on a rubber lifter or tape, keep the original ground the print is on, and copy the print using digital technology. Ideally, from a crime-solving perspective, it is hoped the interconnected nature of our society will eventually lead to having all fingerprint databases linked for easy cross-reference. However, there are several issues to be dealt with, such as funding, jurisdictional bickering, security and privacy to consider before such a fingerprint system can exist [1, 2, 3].

Fingerprint Recognition System is a free tool that will recognize and verify fingerprints. Fingerprint recognition identifies people by using the impressions made by the minute ridge formations or patterns found on the fingertips. Finger printing takes an image of a person's fingertips and records its characteristics - whorls, arches, and loops are

recorded along with patterns of ridges, furrows, and minutiae. Information is processed as an image and further encoded as a computer algorithm [4, 5, 6].

2. Related works

Munir M. A.*et. al.,*[7] presented a fingerprint matching scheme that utilizes a ridge feature map to match fingerprint images. The technique described here obviates the need for extracting minutiae points to match fingerprint images. The proposed scheme uses a set of 16 Gabor filters, whose spatial frequencies correspond to the average inter-ridge spacing in fingerprints, is used to capture the ridge strength at equally spaced orientations. A circular tessellation of filtered image is then used to construct the ridge feature map. This ridge feature map contains both global and local details in a fingerprint as a compact fixed length feature vector. The fingerprint matching is based on the Euclidean distance between two corresponding feature vectors. Basca C. A. *et. al.,*[8]introduced a method of optimizing Gabor Filter Banks using an evolutionary approach. Texture segmentation has multiple usages from medical imaging to satellite terrain mapping. Gabor filters are the most widely used texture feature extractors. Multi-channel approach to texture segmentation using Gabor filters is subject to optimization. Genetic algorithms are used to generate an optimal filter bank for the source image. Malathi, A.***et. al.,*** [9]used a clustering/classify based model to anticipate crime trends. The data mining techniques are used to analyze the city crime data from police department. The results of this data mining could potentially be used to lessen and even prevent crime for the forth coming years. Malathi, A***. et. al.,*** [10] discussed that a major challenge facing all law-enforcement and intelligence gathering organizations was accurately and efficiently analyzing the growing volumes of crime data. There is an enormous increase in the crime in the recent past. They looked at outlier detection algorithm with some enhancements to aid in the process of filling the missing value and identification of crime patterns. They applied these techniques to real crime data and use semi-supervised learning technique here for knowledge discovery from the crime records and to help increase the predictive accuracy. Rai R*., et. al.,*[11]described a fingerprint recognition system consisting of three main steps-fingerprint image preprocessing, feature extraction and feature matching by two different processes. First processes were based on Gabor filter and second was based on FFT (Fast Fourier Transform) filter. We used this process in the fingerprint image preprocessing steps and after getting result by first step then used feature extraction and feature matching steps simultaneously and separately for each process. After applying all the steps, we calculated the FAR (False Accept Rate) and FRR (False Reject Rate) for both processes separately and compare results on the basis of FAR and FRR of Gabor filter based and FAR and FRR of FFT Filter based. Mande, et. al., [12]introduced binary clustering and classification techniques were

used to analyze the criminal data. The crime data considered from Andhra Pradesh police department that aimed to potentially identify a criminal based on the witness/clue at the crime spot an auto correlation model was further used to ratify the criminal. Hashem, et. al.,[13]introduce genetic algorithm as a tool to select optimal fingerprint, master fingerprint, which in their point of view present the most universal image which include more detailed features to recognition. Master fingerprint will be feature's vector which stored in database and will be depended for investigation.

3. Proposal of Criminal Investigations Advanced by Fingerprint Recognition

For the crime database, various data fields were identified to cover real world scenarios. The entities that were identified in our proposal only are Criminals (Suspect and Convict). So we see any crime investigation highlights primarily on one direction of the crime; this is criminal direction. For the criminals we select the most critical attributes (variables) are very interested and repeated in crime registration. The criminal direction is a dataset has it is own attributes are two classes, Informatics and Bioinformatics:

- Information Attributes: this is the first class of criminal which is present most of important attributes related to analyze and investigate the crimes depending on what information available about criminals, these attributes are: Criminal identified, Criminal gender, Criminal age, Criminal address, Criminal income, Criminal job, Criminal marital stat use, Criminal signs difference, Criminal religion, Criminal national, Criminal weapon, Criminal victim, Criminal witness.
- Bioinformatics Attributes: this is the second class of criminal which is concentrate on get optimal fingerprint for the criminals so even they try to alternate their fingerprint we could discover that by the modest proposal of fingerprint recognition using genetic algorithms

The Proposed Fingerprint Recognition for Criminals investigation

Now will explain the proposal tend to strength fingerprint recognition to overcome on alternations of criminal fingerprints. There are many points must be considered in account for avoiding the failure and unreliability of the system, these are summarized as follow:

Direct matching between the fingerprint pattern to be identified and many already known patterns has problems due to its high sensitivity to errors such as various noises, damaged fingerprint areas, or the finger being placed in different areas of fingerprint scanner window and with different orientation angles, finger deformation during the scanning procedure. A single registered fingerprint may have 100 or more identification points that can be used for identification purposes. There is no exact size requirement as the number of points found on a fingerprint impression depends on the location of the print. A good reliable

fingerprint processing technique requires sophisticated algorithms for reliable processing of the fingerprint image: noise elimination, minutiae extraction, rotation and translation-tolerant fingerprint matching. The algorithms must be fast for comfortable use in applications with large number of criminals. Fingerprint weaknesses, requires careful enrollment, potential high False Reject Rate (FRR) due to: pressing too hard, scarring, misalignment, dirt. Here will introduce the proposed framework of fingerprint recognition in generic steps of algorithm, and then explain each step separately.

Algorithm: Proposed Framework of Fingerprint Recognition

Input: database of fingerprints images of criminal persons each one have 10Fingerprints.

Output: Fingerprint recognition system with high quality.

Initialization: Image specifications are 8-bit gray scale (256 levels), 500 dpi resolution, (1-by-1) inch size.

Process:

Step1:*Enrollment*, for each person input the 10 fingerprints image into the following consequences steps to select optimal fingerprint feature's vector to accomplish the enrollment,

1. ***Image preprocessing***, enhancement using histogram equalizer.
2. ***Apply rough segmentation using Gabor filter***, here the aim is to extract the global features, global patterns (plain arch, tended arch, left loop, right loop, and whorl).
3. ***Image Binarization*** will binarized images so that it will be in black and white (matrix of zeros and ones elements).
4. ***Apply soft segmentation for*** findinginteresting area of the image what is called region of interest (ROI). It presents the preliminary step of thinning process.
5. ***Thinning is*** how the ridges will reduce into 1 pixel so that the useful and useless ridges will be clear. Here the aim is to extract the local features; local patterns (Minutia features).
6. ***End For***

Step2: Build proposed vectors and applying proposed Genetic Algorithm, each vector will consist of both patterns of global features obtained by Gabor filter and patterns for Minutia obtained by thinning so will get 10 vectors. Then apply GA to optimize a solution, to get optimal vector which present full description of fingerprint global and local features.

Step3: Identification, Recognition and matching, when some of criminal persons entered his fingerprint image, this image will enhanced, rough segmented by Gabor filter, binarized, soft segmented to find ROI, finally thinned. All that to build it is vector to match it with identical stored vector of that criminal person.

End of Process

3.1. Enrollment

Now will begin with fingerprint database enrollment process, the last process have consequence steps (from enhancement to feature extraction) will be introduced in the following subsections. Enter 10 fingerprints for one criminal. For each 10 image will apply the following image processing steps, figure 1 present one of ten images of criminal fingerprint.

- ***Fingerprint Image Enhancement,*** Enhancement for the 10 fingerprint image will perform using some algorithms, the proposal will use Histogram equalization, see figure 2, to spread pixels of an image so that it will fill the pixel values distribution of an image to increase the perceptional information. This step will introduce enhanced image using Histogram equalization. The enhanced image then will take the range from 0 to 255 pixels.

- ***Fingerprint Image Rough Segmentation,*** Fingerprint images may have background information that does not represent the fingerprint itself. Segmentation removes the background information and is the effective step in the pre-processing of the fingerprint image. A Gabor filter is linear filter whose impulse response is defined by a harmonic function multiplied by Gaussian function. The Fourier transform of a Gabor filter's impulse response is the convolution of Fourier transform of harmonic function and the Fourier function of Gaussian function. g(x, y) = s(x, y) w_r (x, y), where s(x, y) is a complex sinusoidal, known as the carrier, and w_r(x, y) is a 2-D Gaussian-shaped function, known as the envelop. The general function of Gabor filter can be represent as [],

$$G(x,y,\theta,f_0)=\exp\left\{-\frac{1}{2}\left(\frac{x_\theta^{\,2}}{\sigma_x^2}+\frac{y_\theta^{\,2}}{\sigma_y^2}\right)\right\}.\cos(2\pi f_0 x_\theta), \quad (1)$$

$$\begin{bmatrix} x_\theta \\ y_\theta \end{bmatrix}=\begin{bmatrix} \sin\theta & \cos\theta \\ -\cos\theta & \sin\theta \end{bmatrix}\begin{bmatrix} x \\ y \end{bmatrix} \quad (2)$$

…… (1) and (2) [11]

where θ is the ridge orientation with respect to vertical axis, f_0 is the selected ridge frequency in xθ – direction, σ_x and σ_y are the standard deviation of Gaussian function along the xθ and yθ axes respectively and the [xθ, yθ] are the coordination of [x,y] after a clockwise rotation of the Cartesian axes by an angle of (90-θ). Referring to the function in (1), the function $G(x,y,\theta, f_0)$ can be decomposed into two orthogonal parts, one parallel and the other perpendicular to the orientation θ.

$$G(x,y,f_0)\big|_{\theta=90^\circ}=G_{BP}(x,f_0)G_{LP}(y)$$

$$G_{BP}(x,f_0)=\exp\left\{-\frac{1}{2}\left(\frac{x^2}{\sigma_x^2}\right)\right\}\cos(2\pi f_0 x)$$

$$G_{LP}(y)=\exp\left\{-\frac{1}{2}\left(\frac{y^2}{\sigma_y^2}\right)\right\}$$

……(3) [11]

where G_{BP} is only a band-pass Gaussian function of x and f_0 parameters while G_{LP} is only a low-pass Gaussian filter of y parameter. This step will introduce peace of fingerprint image (center) after applying Gabor method on it and also

present Gabor visualization for this image (figure 3).

- ***Fingerprint Image Binarization,*** Gray scale image will binarized, so that it will be in black and white (matrix of zeros and ones elements) the binarization will done by choosing carefully a threshold value where the values for image matrix over the threshold value will become 1 (black) and values less than threshold will be 0 (white), binarization show the minutiae in the image (figure).

- ***Fingerprint Image Soft Segmentation.*** After binarization a segmentation for the image will done where the interesting area of the image identified and as what we call region of interest (ROI), there are two steps for segmentation was Block directionand the second step was identifying the region of interesting. Block direction(figure 5), considering the block direction was done by calculating the x-direction and y-direction for a given block this done by using sobel filter and calculating the gradient value by formula.

$$tg2\,\theta = 2\sin\theta\cos\theta\,/(\cos2\theta - \sin2\theta)\ldots\ldots\ldots (4)$$

the formula is to calculate x-direction and y-direction for each block and consider them as sine and cosine values, when that done for every block we could got blocks with useful information so that no ridges and furrows in the region as a result we shall remove them. The following formula is for discovering and discarding the unnecessary blocks,

$E = \{2\sum\sum (gx*gy)+\sum\sum (gx2-gy2)\}/ W*W*\sum\sum (gx2+gy2)$ …….. (5) [11]

Where if E is under a certain threshold value then the block is considered as a back ground block not belongs to the fingerprint.

Region of Interest(figure 6),after specifying the valuable direction we used the 'OPEN' and 'CLOSE' to present that region, the 'OPEN' operator is to show the new image and cut off the peaks in background, where the 'CLOSE' operator was to reduce the image so that removing the small cavitations. By subtracting the close area form the open area will got a bound area and inner area.

- ***Fingerprint Image Thinning,*** in thinning stage the ridges will reduce into 1 pixel so that the useful ridges will be clear and the useless ridges will clear also. An advantage of this method is that it doesn't produce a discontinuity on the lines, the algorithm is deleting points that lie outer boundaries of the ridge where the width is longer than one pixel but if that may cause a disconnectivety on the graph the pixel will not be deleted (figure 7).

The thinned image may contain some unnecessary spikes and breaks which may lead to recognition of false minutiae those spikes and breaks should be removed in order to extract the minutia, as in traditional, if an angel comes with a

branch and ridge is larger than the 70 degrees and less than the 110 degrees, and if the length of the branch is less than the 20 pixel so that this branch will be removed. Also if a break in some ridge is less than 15 pixels and no other ridges will pass through it, then this break will connected. Aligning minutia, in windows is to decide making minutia as bifurcation or termination. For the matrix that will be saved, the following steps are prepared: present the each bifurcation as three terminations, each termination will be presented by three elements: x-coordinate, y-coordinate, and orientation, see figure (8).

3.2. The Proposed Genetic Algorithm to Select Optimal Feature's Vector From all above we can say the proposal apply two levels of segmentations, these are:

1. Rough segmentation which done by Gabor filter, from this segmentation extract the global patterns of fingerprint (plain arcs, tented arcs, left loop, right loop, and whorl).
2. Soft segmentation which done by there are two step for segmentation is block direction and the second step is identifying the region of interesting followed by thinning, from these three steps will extract local patterns of fingerprint (miniature).

Build vectors are constructing the population of GA; each vector will contain both global patterns and local patterns. To apply a genetic algorithm for solving problem of selecting master fingerprint from one class, this research proposes to define or to select the following component:

Note: oi represent symbol of global patterns and pi represent symbol of local patterns.

1. A genetic representation or encoding schema for potential solutions to the problem, here each fingerprint will be presented as a vector each vector consist from the following:

(*no. of global pattern, (o1, (position (x, y coordinates), orientation, texture, object shape and topology), o2(…..), on(……), no. of local patterns, (p1, (position (x, y coordinates), orientation, texture, object shape and topology), p2(…..), pn(……)*).

2. A way to create an initial population of potential solutions, the initial population already created with image processing algorithms which established the vectors. So this mean the initial population of each 10 criminal's fingerprint, will be these 10 images represented by vectors.
3. An evaluation function that plays the role of the problem environment (best fingerprint), rating solutions in terms of their "fitness". Here the proposed evaluation function for each fingerprint is ***f(vector) = (no. of object + ∑ (features of each objects))***.
4. Genetic operators that alter the composition of offspring. *One-point crossover* is the most basic crossover operator, where a crossover point on the genetic code is selected at middle of vector which separate global and local

features, and two parent vectors are interchanged at this point.

5. Crossover exploits existing vectors potentials, but if the population does not contain all the encoded information needed to find the best vector, no amount of vector mixing can produce a satisfactory solution. For this reason, a mutation operator capable of spontaneously generating new vector is included. The most common way of implementing mutation is to flip some feature with a probability equal to a very low, given mutation rate (MR). A mutation operator can prevent any single feature from converging to a value through the entire population and, more important, it can prevent the population from converging and stagnating at any local optima.
6. Values for the various parameters that the genetic algorithm uses population size, rate of applied operators, etc..In our particular problem we use the following parameters of the genetic algorithm: Population size, *pop-size* = 10 (the parameter was already used), Probability of crossover, PC = 1, Probability of mutation, PM = 0.001 (the parameter will be used in a mutation operation).
7. Continue with genetic processing until obtain the optimized vector to be the master vector.
8. Order the other nine vector according their nearest from the master vector and store them as a measure in some suspected instances of recognition.

3.3. Identification, Recognition and Matching

After accomplishing the six steps above, the enrollment would be accomplished. When enrollment performed for all criminal persons, the system of fingerprint recognition will be ready to recognize images of fingerprint criminal or not. Recognition process depend on method used in matching, matching will done when some of criminal persons entered his fingerprint image, this image will submitted to the five consequence image processing enhancement, rough segmentation by Gabor filter, binarization, soft segmentation to find Block Direction and ROI, finally thinning. All that to build it is vector to match it with corresponding stored vector of that criminal person.

Fingerprint matching will applied in this research is based on finding the Euclidean distance between the corresponding feature vectors (entered and stored). The Euclidean distance of the vector of the entered fingerprint image and vector of corresponding stored can be calculated as follows,

$$\varepsilon = || \Omega - \Omega_k || \quad \ldots\ldots\ldots \quad (6)$$

where Ω kis a vector of stored fingerprint. When get a minimum score that belong to the best alignment of the two fingerprints being matched? If the Euclidean distance between two feature vectors is less than a decided threshold, then the decision that the two fingerprint images come from the same finger, otherwise a decision that the two

fingerprint images come from different fingers.

4. Experimental Works and Results

In this proposal since we deal with crime domain the data are so sensitive and not be ready available for us, for that from our environment as teachers we assume 50 student as criminal and depend on 500 fingerprint images for 50 student (as criminal), so each criminal will has 10 images. Enrollment process will do for all these 500 images to finally detect the master image for each person and other nine nearest images. So there are two databases in this enrollment: preliminary and secondary. Preliminary will store master images vectors, which has in our experimental just 10 vectors. Secondary will store the most nearest vector to the master vector, which will used in uncertainties cases. The matching stage must be flexible because 100% match may never occur, for that the matching stage is depending on determined a threshold value, in our proposal will give 98.5% -98% as a threshold, so if the two global patterns or two local patterns is in a box and no scaling for them they are matched. In traditional matching score calculated as in the following equation,

$$\text{Matching Score} = \frac{\text{Number of minutia pairs that match}}{\text{Total number of minutia pairs}}$$

…… (7)

In our proposal will as in follow,

$$\text{Matching Score} = \frac{\text{Number of global pairs and local pairs that match}}{\text{Total number of global pairs and local pairs}}$$

…… (8)

In both traditional and proposal there are the two probabilities these are: two fingerprint from two different persons may produce a high Matching Score (an error); two fingerprints from the same person may produce a low Matching Score (an error). So as usual in all systems there are **two types of error**: **FAR** = ratio of number of instances of pairs of different fingerprints found to (erroneously) match to total number of match attempts.

$$FAR(n) = \frac{\text{Number of successful independent fraud attempts against a person n}}{\text{Number of all independent fraud attempts against a person n}}$$

…… (9)

FRR = ratio of number of instances of pairs of same fingerprint are found not to match to total number of match attempts.

$$FRR(n) = \frac{\text{Number of rejected verification attempts for a qualified person(or feature)n}}{\text{Number of all verification attempts for a qualified person(or feature)n}}$$

…… (10)

The performance of a fingerprint recognition system can be evaluated by measuring its false reject rate (FRR) and false accept rate (FAR). By evaluating the FRR and FAR, the threshold of matching score deciding whether to reject or accept a match is set to optimizing the performance. If we take less threshold value it means the probability of

accepted image will be high and rejected image will be low and due to this, chances of occurring error will be increased and vice versa. Our obtained simulation results are shown in table (1).

5. Conclusions

In our previous work [13], we introduce the proposal of enhance fingerprint recognitions using genetic algorithms without any applicable domain. Here, the proposal applied in a very sensitive and important field it is the criminal investigation, where the most of the criminals try to alternate their fingerprint, so we introduce our proposal in which depend on an idea to optimize feature's vector of fingerprint image that by taking several impressions for one person in different circumstances that to consider all features may be losses in some cases of person's impressions or in some cases of alternation. GA was a good tool for optimizing features vector among 10 vectors for each person. Using Gabor filter in rough segmentation level enhance the extractions of global pattern features. The reason for increase accuracy of the proposal belongs to considering both patterns ridges and minutiae in calculating matching scores. Our proposal calculates the results FAR and FRR with two thresholds to ensure of proposal accuracy as shown in table (1).

Figure1. Source fingerprint image

Figure2. After histogram

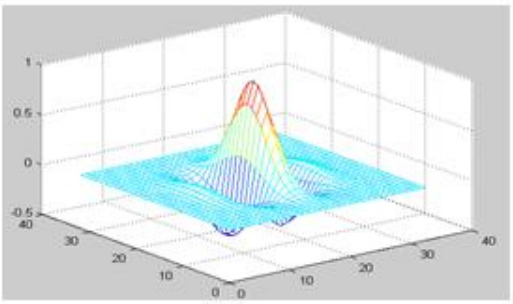

(a)

(b)

Figure3.a-Gabor visualization for an Fingerprint image, b- Enhanced fingerprint image.

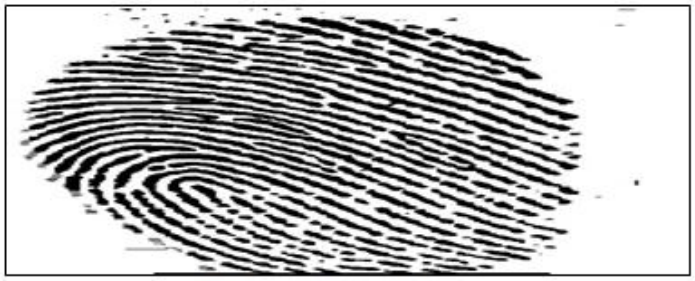

Figure4. Binary image

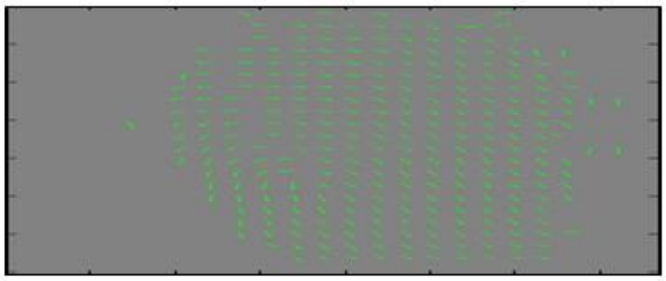

Figure5. Block direction

Figure6. Region of Interest

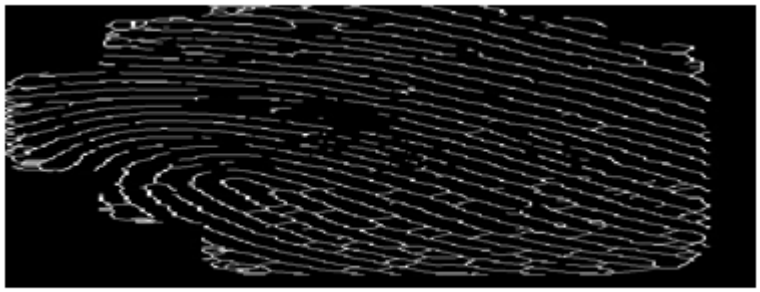

Figure7. Thinning

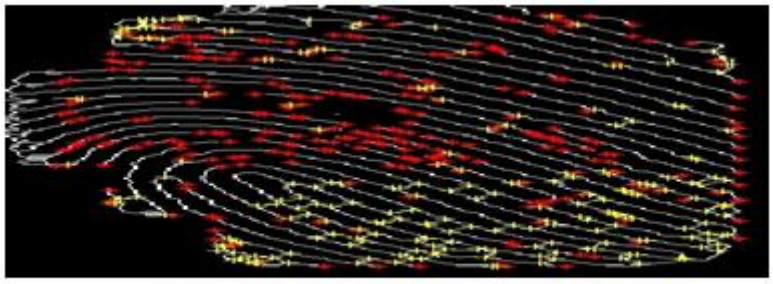

Figure8. Extract minutia from the fingerprint

Table 1. FAR and FRR with traditional, proposal [13] and applicable proposal.

Recognition System	FAR Threshold # 98%	FRR Threshold# 98%	FAR Threshold# 98.5%	FRR Threshold# 98.5%
Traditional	0.95%	23.11%	0.84%	24.41%
Proposal [13]	0.22%	15.57%	0.11%	15.98%
Applicable Proposal of Criminal	0.20%	14.25%	0.10%	14.67%

References

1. Barnard, A. Fingerprints - How Fingerprints Solve Crime, IICFIP Conference, www.IICFIP.Org.
2. Ross, A., Jain, A., AndReisman, J. (2003) A Hybrid Fingerprint Matcher, Pattern Recognition 36, 7: 1661 1673.
3. Jea T., Chavan V. K., Govindaraju V., Schneider J. K. (2004) Security and matching of partial fingerprint recognition systems. In Proceeding of SPIE, Number 5404: 39–50.
4. Maltoni, D., Maio, D., Jain, A.K., Prabhakar, S. (2003) Handbook of fingerprint recognition, New York, Springer.
5. Nawaj T., Parvaiz, S., Korrani, A., Din, A-d. (2009) Development Of Academic Attendance Monitoring System Using Fingerprint Identification", International Journal Of Computer Science And Network Security (IJCSNS), 9:164-168.
6. Huang P., Chang C. Y., Chan C. (2007) Implementation of an automatic fingerprint identification system, IEEE, EIT: 412-417, 2007.
7. Munir, M.U., Javed, M. Y, (2004) Fingerprint Matching Using Gabor Filters, National Conference On Emerging Technologies 2004 College Of Electrical And Mechanical Engineering, National University Of Sciences And Technology Rawalpindi, Pakistan.
8. Basca, C.A., Blaga, L. (2007) Texture Segmentation. Gabor Filter Bank Optimization Using Genetic Algorithms. Http://Rbrad.Ulbsibiu.Ro/Publications/Papers/EUROCON2007.Pdf.
9. Malathi, A., Baboo, S.S., Anbarasi A. (2001) An Intelligent Analysis Of A City Crime Data Using Data Mining, 2011 International Conference On Information And Electronics Engineering, IPCSIT Vol.6 (2011) © (2011) IACSIT Press, Singapore.
10. Malathi, A., Baboo, S.S. (2011) Enhanced Algorithms To Identify Change In Crime Patterns, Int. J. Combinatorial Optim. Problems Informatics. 2(3): 32-38.
11. Rai R., Rai, A.,Bagla, Singhal, A. (2011) Comparative Analysis Of Gabor Filter And Ftt Filter Based Fingerprint Recognition System. Int. J. Information Technol. Knowledge Management. 4 (1): 177-180.
12. Mande U., Srinivas Y. And Murthy J.V.R. (2012) An Intelligent Analysis Of Crime Data Using Data Mining & Auto Correlation Models. Int. J. Eng. Res. Applications. 2(4): 149-153 149.
13. Hashem S. H., Maolod A. T., Mohammad A. A. (2013) Proposal To Enhance Fingerprint Recognition System. Int. J. Computer Eng. Technol. 4(3).

Effect of Crude Extract of Saponin of Seeds Sesbania Sesbon on Cholesterol Level in Blood of Mice

Athraa Hussein Ali

Department of Biology, College of Education Ibn- AL Heitham

University of Baghdad

Ph. 00964 7811332431

Abstract

The current Study was carried out to determine the effect of different concentrations (0.03, 0.06, 0.12, 0.25) of crude extract of saponin seeds Sesbania sesbon (L) Merrill on the haemolytic activity of saponin on red blood corpuscles under laboratory conditions. Results indicated that percentage of haemolysis was 100% at concentrations 0.12 and 0.25 of saponin but the activity of saponin blocked by adding different concentrations (0.2, 0.4, 0.6, 0.8, 1) % of cholesterol. Thus, negative relationship was found between haemolytic activity of saponin and cholesterol concentration. No observable lysis was found at 1% of cholesterol. The effect of sesban saponin extract on the cholesterol level of mice blood at different time intervals (4, 8, 12 hours) post injection showed decrease in cholesterol level when increased saponin concentration with decreasing the period of injection. The lowest level of cholesterol observed in mice that injected with 0.12 and 0.25 of saponin after 4 and 8 hour of injection.

Keywords: Saponin, cholesterol, haemolysis.

تأثير المستخلص الخام لسابونين بذور نبات السيسبان على معدل الكوليسترول في دم الفئران البيض

عذراء حسين علي - كلية التربية ابن الهيثم / قسم علوم الحياة - جامعة بغداد

الخلاصة :

تم دراسة تأثير تراكيز (0.03 ، 0.06 ، 0.12 ، 0.25) للمستخلص الخام للسابونين من بذور نبات السيسبان *Sesbania sesbon* (L) Merrill على الفعالية التحليلة لكريات الدم الحمراء .أظهرت النتائج ان نسبة التحلل كانت 100% في التراكيز (0.12 ، 0.25) ، في حين ثُبط تأثير السابونين بأضافة الكوليسترول بتراكيز مختلفة (1 ,0.8 ,0.6 ,0.4 ,0.2)% فوجدت علاقة عكسية بين فعالية السابونين التحللية من جهه ونسب الكوليسترول من جهه أخرى، فكانت نسة التحلل صفر % بتركيز 1% كوليسترول، اما تأثير السابونين على معدل الكوليسترول في دم الفئران بعد (4, 8, 12)ساعة من الحقن فقد لوحظت زيادة واضحة في أنخفاض مستوى الكوليسترول كلما زاد تركيز السابونين المستخدم وقلة فترة الحقن فبلغ أوطا معدل للكوليسترول في التراكيز (0.12 ، 0.25) للسابونين بعد (8,4) ساعات من الحقن .

الكلمات المفتاحية :سابونين ، كوليسترول ، تحلل

Introduction

Steroid sapogenins have till now been found only in higher plants which named as secondary product [1]. These compound were named because they have no obvious metabolic function and their very diversity of structure and distribution among living organisms [2]. The aqueous solution of saponin which form foam like soap[3], saponin has a more or less strong haemolysing effect on blood erythrocytes in vitro [4]. The effect was showed that after diet containing well soybean saponin were fed rats and mice nor saponin could be found in the blood stream of the test animals, this showed that no saponin had been absorber through digestive tract [5]. Cholesterol is widely distributed in all cells of the body but particularly in nervous tissue, it is the parent compound of all steroids synthesized in the body. It occurs in animal fats but not in plant fats [6]. Many investigators have demonstrated a correlation between raised serum lipid levels and the incidents of coronary heart disease and atherosclerosis in human [7], of the serum lipids. Cholesterol has been the one most often singled out as being chiefly concerned in the relationship of the factor that lower blood cholesterol, the substitution in the diet of poly unsaturated fatty acid for some of the saturated fatty acids has been the most intensely studied, naturally occurring oils are beneficial in lowering plasma cholesterol include pear rut cotton seed, corn and soybean [8].

Material and methods

Sesbania saponin was extracted (SSE) from seed of sesbania sesban (L.) Merrill. It was prepared from ether extracted sesbania flour [9]. haemolytic activity of saponin on red

blood corpuscles (RBC) has been studied by dissolving saponin extract in physiological saline (0.85% Nacl) to give a concentration of 10 mg/ml, the erythrocytes were prepared by centrifuging mice blood at 6,000 g for 5 min to remove the supernatant, after washing the collected (RBC), 20 ml RBC was added to 80 ml saline to give 2% erythrocyte suspension. To determine haemolytic activity five test tubes were used, for rep (0.25) ml dissolved extract was added to tube 1, tubes 2-5 that containing 0.25 ml physiological saline to tube 2 added 0.25 ml dissolved saponin extract. Series dilutions were made by transferring 0.25 ml of the dilution to tube 3, mixed well and then transferring (0.25) ml to tube 4 and the last tube was used as a control without added saponin extract. To all test tubes 0.25 ml of mice red corpuscles was added. As a result of the dilutions these concentra-tions of saponin per ml of water existed in tubes 1-5 (0.25, 0.12, 0.06, 0.03, 0 %). Test tubes were shaken to mix the contents, incubated at room tempera-ture (1 hour) then observed for haemolysis .When complete haemolysisoc-curred the tubes showed a uniform cherry-red from the hemoglobin released from disrupted red blood corpuscles. In partial haemolysis, the saline ap-peared pink and unlysis corpuscles had settled to the bottom of the tubes, and the saline was clear. To study the ability of cholesterol for depressing the effect of SSE for haemolytic activity could be overcome by adding cholesterol to blood at concentrations (0.2, 0.4, 0.6, 0.8, 1%) to each concentration of saponin.

Animals and Experimental design

SSE and cholesterol were given to five groups of white mice (albino mice - Musmusculus /Balb 1/C strain) weights ranged between 25-28 gm each group consist 4 boxes distributed in the form of square (4 x4), three mice (28-31 day old) and the same weight were put in each box, the boxes were placed in a constant temperature of room (23°±1°) the tails of mice were injected with SSE at concentrations (0.03, 0.06, 0.12, 0.25%) were anaesthetized by chloroform and wrapped in a saran net and the blood was taken by cutting the tail. The blood of every three mice of the same cage was put in one test tube and the level of cholesterol was determined after 4, 8, 12 hours.

Results and Discussion

Haemolysis of erythrocyte has been used to demonstrate the haemolytic activity of saponins with or without addition of cholesterol. The data in table 1 indicated that SSE at zero% of cholesterol showed the highest haemolysis at concentrations 0.12 and 0.25% of saponin, while addition of cholesterol at 0.4% caused partial haemolysis at concentrations of 0.12 and 0.25% of SSE, thus, haemolytic activity decreased gradually with increased the cholesterol concentration to reach zero % at 1% concentrations of cholesterol. Thus, haemolyticactivity of saponins on red blood corpuscles are probably caused by lipoid-protein constituents penetrating the membrane surface [10]. Activity of saponins may dissolve fatty materials or may denature proteins in the cells surfaces, leaving holes sufficiently large for hemoglobin molecules [11]. This is also supported by [12], recognized that certain chemicals such as benzene, toluene and saponin, which are fat – solvents may act on the red corpuscles membrane and disrupting the lipid components. The effect of SSE on the cholesterol level of mice blood was

summarized in table 2. From the table, it can be seen that the reversal relationship between SSE and cholesterol which appear decrease after 4 and 8 hours of injection, while the effect disappear after 12 hour. The lowest percentage of cholesterol reach at 0.25% concentration of SSE after (4,8) hour were 129.84 and 133.73 mg/100 ml respectively. While, at 0.03% of SSE, the percentage of cholesterol relatively equal to control 157.01, 156.90, 160 mg/100 ml at 4, 8, 12 hour, respectively. Highly signification differences could be found between control groups and SSE concentrations at 0.12 and 0.25% and period of injection on cholesterol level in plasma of mice , while no significant found in interaction effect. In fact, decrease of cholesterol level due to complex formed with SSE this is supported directly by previous study [13], that showed saponin has the ability to form complex with lipids [14], this study showed that saponin from an aqueous phase could penetrate into and complex with amber of surface absorbed lipids particularly cholesterol to form very insoluble complexes. The involvement of saponin with cholesterol may lead also to possibility of an interference with other function so a reduction in blood plasma cholesterol occurred when injection of saponin in mice, but organisms sensitive to saponin could react to one or more of the fraction [15]. Further studies are necessary to complete the work.

Table 1. The effect of cholesterol on haemolytic activity of ses ban saponin in vitro.

% Concentration of saponin					
% cholesterol	0	0.03	0.06	0.12	0.25
0	-	±	±	±	+
0.2	-	±	±	±	+
0.4	-	±	±	±	±
0.6	-	-	-	±	±
0.8	-	-	-	-	±
1	-	-	-	-	-

- = 0% haemolysis (no observable lysis)

± = partial haemolysis .

+ = 100% haemolysis .

Table 2. Cholesterol level in plasma of mice

Cholesterol level in plasma of mice mg/100 ml			
% Concentration of saponin	After 4 hour	After 8 hour	After 12 hour
0	158.17	157.43	160.01
0.03	157.01	156.90	160
0.06	139.46	143.63	158.80
0.12	131.30**	136.35**	154.01
0.25	129.84**	133.73**	153.22

** These figures are statistically different at P<0.01 for concentration of SSE and the period after in action

No significant difference in interaction

References

1. Kosmas, H., Miranda, T., Anne, E. (2002) Biosynthesis of triterpenoid saponins in plants. Advances in biochemical engineering/Biotechnology. 75: 31-49.
2. Foerster and Hartmut. (2006) MetaCyc pathway: saponin biosynthesis. New York City: Academic press: 161.
3. Haralampidis, K., Trojanowska, M, Osbourn, A,E. (2002) Biosynthesis of triterpenoid saponins in plants. Advances in Biochemical Engineering/ Biotechnology 75:31-49.
4. Gogelein, H., Huby, A. (1984) Interaction of saponin and diagitonin with black lipid membranes and lipid monolayers. Biochemical Biophysical Acta. 773: 32-38.
5. Zohar F., Harinder P.S., Klaus. (2002) The biological action of saponins in animal system: a review. British J. Nutr. 88(6): 587-605.
6. Synthia, H., Lisa, D. (2002) Neurosteroids: biochemistry and clinical significance. Dept of Neurology, University of California Volume 13, Issue 1: 35–43.
7. Jimenez, M.A., Scarino, M.L., Vignolini, F., Mengheri, E. (1990) Evidence that polyunsaturated lecithin induces a reduction in plasma cholesterol level and favorable changes in lipoprotein composition in hypercholesterolemic rats. J Nutr. 120(7): 659-667.
8. Grundy, S.M., (2002) Comparison of monounsaturated fatty acids and carbohydrates for lowering plasma cholesterol. J. Nutr. 314(12):745.
9. Birk,Y., Bendi,A., Gestetner,B., Ishaaya, T. (1963) Atherme stable haemolytic factor in soy beans. Nutr, Lond. 197, 1089-1090 .
10. Melzig, M.F., Bader, G., Loose, R. (2001) Investigation of the mechanism of membrane activity of selected triterpenoid saponins. Planta Medica. 67: 43-48.
11. Alada, A.R.A., Akande, O.O., Ajayt, F.F. (2004) Effect of soybean diet preparations on some haematological and biochemical indices in the rat. African J. Biomedical Res. 7: 71-74.

12. Iren, B., King, Rozenn, N., Lemaitre, Mark, K. (2006) Effect of a low-fat diet on fatty acid composition in red cells, plasma phospholipids, and cholesterol esters: investigation of a biomarker of total fat intake. Am. J. Clin. Nutr. 83: 227-236.
13. Bangham, A.D., Horbe, R.W., Glauert, A.M., Dingle, J.T., Luoy, J.A. (1962) Action of saponin on biological cell membranes. Nutr.,Lond, 196: 952-955.
14. Baumann, E., Stoya, G., VoÈlkner, A., Richter, W., Lemke, C., Linss, W. (2000) Haemolysis of human erythrocytes with saponin affects the membrane structure. Acta Histochem, 102: 21-35.
15. SchSnbeck, F., Schbsser, E. (1976) Preformed substances as potential protectants, in Physiological Plant Pathology, Heitefuss, R., Williams, P.H., eds: 653-678.

Optimum Conditions of Protease Production from *Bacillus licheniformis*(B1) and its Applications

Haider Jawad Kadhim[1] and Sanaa Burhan Aldeen[2]

[1]Biology Department, College of Science, University of Baghdad (hyder7h@gmail.com)

[2]Biology Department, College of Science, University of Baghdad (salnama@yahoo.com)

Ph. 00964 7811332431

ABSTRACT

Forty isolates of Bacillus spp. were isolated from sixty samples including; soil, water and meat. Ability of these isolates to produce protease was evaluated. Bacillus B1 isolated that isolated from soil showed the highest protease production. it was identified as a strain of Bacillus licheniformis.The optimum culture medium and conditions for protease production were casein-yeast extract medium contained soluble casein (0.5g), yeast extract (0.5g), glucose (1g), KH2PO4 (0.02g), K2HPO4 (0.02g) and MgSO4.7H2O (0.01g), in 100ml distilled water, pH 8.0 and incubated at 37˚C. for 48 h. The crude protease exhibited ability to remove the blood color from cloth within 30 min and gelatin from X-ray film within 120 min.

Keywords: Protease, Production, *Bacillus licheniformis*, applications.

انتاج وبعض تطبيقات انزيم البروتييز من بكتريا *Bacillus licheniformis* B1

حيدرجواد كاظم وسناء برهان الدين

قسم علوم الحياة، جامعة بغداد

الخلاصة:

تم الحصول على 40 عزلة عائدة لجنسBacillus والتي عزلت من 60 نموذج تضمنت عينات تربة و مياه ولحم. اختبرت قدرة هذه العزلات على انتاج انزيم البروتييز، وبينت نتائج الغربلة على ان العزلة Bacillus B1المعزولة من التربة هي الاغرز انتاجا والتي شخصت على انها احدى سلالات Bacillus licheniformis. درست الظروف المؤثرة في انتاج البروتييز، ولوحظ ان اعلى انتاجية تكون عند زرع البكتريا في وسط casein-yeast extract الحاوي على (0.5 g.) كازائين و (0.5 g.) مستخلص الخميرة و (1 g.) كلوكوز و KH2PO4 (0.02g.) و K2HPO4 (0.02g.) و MgSO4.7H2O (0.01g.) لكل 100مل ماء مقطر برقم هيدروجيني 8 وحضنها بدرجة حرارة 37م لمدة 48 ساعة. اظهر الانزيم قابلية في ازالة بقع الدم من القماش عند الحضنه لـ30 دقيقة، وكذلك اظهرالانزيم امكانية أزالة طبقة الجلاتين من افلام اشعة اكس خلال فترة 120 دقيقة.

الكلمات المفتاحية: انزيم محلل البروتين، انتاج، *Bacillus licheniformis*، التطبيقات.

Introduction

Proteases are a group of enzymes that hydrolyze peptide bonds of proteins and break down into polypeptides or free amino acids [1]. Proteases constitute a class of industrial enzymes. They constitute 59% of the global market of industrial enzymes, which is expected to exceed $ 2.9 billion by 2012 [2]. They have got wide range of commercial usage in detergents, leather, food and pharmaceutical industries [3]. One of the most important characteristics that determine the industrial suitability of proteases is their requirement of high pH for optimum enzyme activity [1]. The preferred sources of proteases are microbes because of their rapid growth and the ease with which they can be genetically manipulated to generate new enzymes with altered properties. However, many of the alkaline proteases applied to industrial purposes face some limitations such as low stability towards surfactants and production cost of the enzymes arisen from growth medium [4]. The genus “Bacillus” is an important source of industrial alkaline proteases and is probably the only genus being commercialized for alkaline protease production [5]. Screening of alkaline proteases producing Bacillus spp. from different ecological environments can result in isolation of new alkaline proteases with unique physio-chemical characteristics [6]. It is known that the amount of enzyme produced greatly depend on strain and growth conditions. Therefore, there is a need to the search of new strains of bacteria that produce proteolytic enzymes with novel properties and the development of low cost media .

Materials and Methods

Microorganism

Bacillus licheniformis isolated from soil and identified according to the morphological, microscopic examination and biochemical tests of Logan, and DeVos [7].

Determination of Proteases Production

Two methods were used for production of proteases.

Semi-quantitative method [8]

Skim milk-peptone agar consisted of Skim milk powder 10 g, Peptone 0.5 g, Agar powder 2 g and distilled water 100 ml. the mixture was inoculated for 24 h with old bacterial culture and incubated for 24 h at 40 °C. Clear zone around the spots and underneath the growth indicate protease production. The diameter of colonies and clear zones were measured. The ratio of clear zone diameter to colony diameter was calculated which represents a semi quantitative assay of protease.

2Quantitative method [9].

Ten ml of casein-peptone broth (Peptone 0.5 g, Soluble casein 0.2 g, NaCl 0.5 g and distilled water 100ml) was inoculated with 0.1 of activated bacterial suspension (optical density = 0.3 at 600 nm) and incubated at 40˚C for 24 h. The crude enzyme was extracted by cooling centrifugation for 15 min. Then the enzyme activity and protein concentration was measured in the supernatant.

Assay of Protease Activity

Protease Activity was determined spectrophotometrically according to previous method of Anson [10] with littel modification. Enzyme extracted solution (0.2 ml) was incubated with 1.8 ml of casein solution at 40 °C for 15 min. The blank consisted of 1.8 ml of reaction solution and 3.0 ml of 5 % TCA (trichloroacetic acid) and 0.2 enzyme solution. The reaction was stopped adding 3.0 ml. of 5 % trichloroacetic acid and incubated at 25 °C for 10 min. The mixture was centrifuged by cooling centrifuge (3000 g) for 10 min, then supernatant was separated. Quantity of 2.5 ml of 0.5M Na2CO3 solution was added to 1 ml of the supernatant and 1 ml of Folin–Ciocalteus reagent was added and incubated at 37°C for 20 min. The absorbance (O.D.) at 600 nm was measured. One unit of protease activity was defined as the amount of enzyme required to liberate one µg of tyrosine per minute per ml. under assay conditions.

Determination the optimum conditions of enzymes production.

Effect of different media in protease Production

The bacterial isolate was activated by culturing in nutrient broth and incubated at 37˚C for 24 h. Each 100 ml of different media casein–peptone medium [9], Horikoshii medium (11) and Casein-yeast extract medium [12] was inoculated with 2 ml of bacterial suspension (O.D = 0.3 at 600 nm) and incubated at 37˚C for 24 h. The cells were precipitated by cooling

centrifugation at 3000 rpm. The supernatants (crude enzyme) were assayed for enzyme activity, protein concentration and calculated specific activity, for select the best production medium.

Effect of Incubation Temperature on Enzyme Production

Quantity 100 ml of casein-yeast extract medium was inoculated with 2 ml of activated bacterial suspension (O.D = 0.3 at 600 nm) and incubated at different temperatures (37, 40, and 50 ˚C) for 24 h. The supernatant was assayed for enzyme activity, protein concentration and specific activity .

Effect of Initial pH on Enzyme Production

Hundred militer of casein-yeast extract medium was prepared at different pH values (7.0, 8.0, 9.0 and 10.0) adjusted with 1N HCl and 1N NaOH. The medium was inoculated with 2 ml of activated bacterial suspension (O.D = 0.3 at 600 nm) and incubated at 37 ˚C for 24 h. The supernatant was assayed for enzyme activity, protein concentration and specific activity.

Effect of Incubation Period on Enzyme Production

Hundred militer of casein-yeast extract medium at pH 8 was inoculated with 2 ml of activated bacterial suspension (O.D = 0.3 at 600 nm) and incubated at 37˚C for different time intervals (24, 48 and 72 h). The supernatant was assayed for enzyme activity, protein concentration, and specific activity. All experiments achieved as a duplicated.

Statistical Analysis

The Statistical Analysis System- SAS [13] was used to determine the significant difference between the different parameters. LSD test (Least Significant Difference) at probability level $P \leq 0.05$ was applied to be significant difference.

RESULTS AND DISCUSSION

Isolation of Bacillus

Sixty samples were collected from different sources; soil, water and meat. Forty bacterial isolates were identified as Bacillus spp. according to growth characteristics on nutrient agar and microscopic examination (Table 1). The growing isolates showed a very wide range of colonial morphologies, they varied from moist and glossy to wrinkled texture. Microscopic examination showed Gram positive rod cells, may occur singly, pairs, chains and filaments. Spore forming and spore shapes vary from cylindrical through ellipsoidal to spherical. Spores might be terminally, subterminal, or central position. However, a Gram-stain is sufficient to determine the presence of spores because the spore remains unstainable while the vegetative cells or the vegetative part of the spore will stain [14].

Screening for protease producing Bacillus

Semi-quantitative screening

Proteolytic activity was assayed using skim milk-peptone agar and expressed as diameter of clear zone to diameter of colony (Table 2). A clear zone of skim milk hydrolysis gave an indication of protease producing organisms [15]. Bacteria are the most dominant group of protease producers with the genus Bacillus being the most prominent and serve as an ideal source of this enzyme [9]. Due to their rapid growth and limited space required for their cultivation [16].

Quantitative screening

According to the previous results seven isolates were selected for quantitative screening of protease production (Table 3). The difference in the production of enzyme from isolates might be due to different source of the isolate or the variation in genes codes protease synthesis [17]. Assay of protease activity is depended on ability of casein hydrolysis thus casein containing medium is used to detect the protease producing microorganisms [12].

Identification of Bacillus B1 isolate

Morphological and physiological properties of the selected isolate was investigated. Relying on the results it can be concluded that B1 isolate is belongs to B. lichenoformis depending on "Bergey's Manual of Systematic Bacteriology [7] (Table 4). *B. licheniformis* is spore former bacteria give positive results in VP-test and catalase [18]. Slepecky and Hemphill [14] mentioned that B. licheniformis has the ability to grow at 40˚C. and 50˚C. This species is used in a wide range of industrial processes, including production of enzymes such as protease [19].

Effect of culture conditions on protease production

Effect of medium compositions

B. licheniformis B1 was cultivated in different media then enzyme production was assayed Results in figure (1) indicated that the casein-yeast extract medium was the best for protease production. Glucose was found to be the optimum carbon source for protease activity by all Bacillus spp. [20]. From nutritional aspects glucose plays an essential role as enzyme inducer for B. subtilis strains [21]. Good protease activity was also observed with B. cereus isolates in media supplemented with glucose [22]. The organic nitrogen compounds support the growth and biosynthesis of protein, nucleic acid and other cell constituents [23]. Martins and Teodoro [24] found that the addition of yeast extract to the liquid medium shortened the lag period and increased the enzyme synthesis. The effect of various metal ions on protease production was reported, supplementation of Mg^{2+}, Ca^{2+} and K^{+} salts to the culture medium exhibited slightly better production [25].

Effect of incubation temperature on enzyme production

Protease activity was assayed at various incubation temperatures (30, 37, 40 and

50 ˚C). The result showed that the best temperature for protease production by B. licheniformis B1was at 37˚C. (Figure 2). Temperature is one of the most important factors affecting the enzyme production [22]. Ray et al. [26] reported that temperature could regulate the synthesis and secretion of extracellular protease by microorganisms. The results of this experiment on Bacillus licheniformis B1 are in agreement with other literatures on alkaline Bacillus strains producing alkaline proteases [27] .

Effect of pH of medium on enzyme production

To investigate the effect of initial medium pH on protease production, B. licheniformis B1 was grown in casein-yeast extract medium with different pH values, the results showed that the enzyme was produced over pH ranged from 7.0 to 10.0 the a maximum value and of specific activity 5.5 U/mg protein, was observed at pH 8.0 (Figure 3). The most important characteristic of microorganisms is their strong dependence on the extracellular pH for cell growth and enzyme production [28]. Mona, [29] found that the maximum protease production could be achieved by controlled pH and temperature. Most of the proteases produced by genus Bacillus exhibit alkaline pH ranged from 8.0-10.0 [30] .

Effect of incubation period on enzyme production

The protease production by B. licheniformis B1 was observed after 24, 48 and 72 h of incubation period the results revealed that the maximum activity (6.1 U/mg) was obtained after 48 h. (Figure 4). It might be conclude that protease is produced during logarithmic phase and reaches its maximum value at stationary phase [31]. Enzyme production in culture medium did not change in the stationary phase and decreased after 32 h. of cultivation [32]. Other studies also suggested that incubation for 48 h was the best incubation time for extracellular protease production by Bacillus sp. [1], B. licheniformis Lbbl-11 (33), B. licheniformis SH-2 [20].

Some applications of protease.

Removing blood color.

The blood stain was removed from pieces of cloth cotton after incubating the cloth in crude protease from B. licheniformis B1 for 30 min (Figure 5) this illustrated showed a good efficiency as compared with control. This result is confirmed the potential application of this enzyme in the detergent industry as additives [34]. Nadeem et al., [35] studied the high capacity of blood stain removal by protease of B. licheniformisN-2. Gehan et al., [36] found that gradual removal of blood stain by increasing the contact time intervals from 10 to 50 min with the enzyme solution .

Vishalakshi et al., [37] reported that blood color is completely removed from the cloths after rinsing with a combination of detergent and partially

purified enzyme for a period of 20 min and it was removed after 25 min when rinsed with partially purified enzyme alone .

Removing of gelatin from X-ray film

The gelatin coating X-ray film was removed by crude protease of B. licheniformis B1 after incubating at 30 °C for two hours (Figure 6). The enzyme when added to X-ray films removed the layer of gelatin and film became transparent [38]. In this study the hydrolysis of gelatin was relatively slow, probably duo to slow adsorption of protease on to the surface of films. Or maybe the concentration of protease as crude was low. Moreover, the incubation temperature (30 °C) may be below the optimum for activity of this enzyme for hydrolysis gelatin. Vijayalakshmi, et al., [39] experimented the efficiency of partially purified protease to hydrolyze the gelatinous coating on X-ray film, where incubated with X-ray films, the hydrolysis was completed within 30 min .

Conclusion

The local isolate of B. licheniformis B1 is an efficient protease producer. Casein-yeast extract medium was the best medium for protease production by B. licheniformis B1 in alkali environment (pH 8) after incubation at 37 C° for 48 h. Protease exhibited potential ability through removing blood stain from cloth and gelatin from X-ray film.

Table 1: *Bacillus* isolates obtained from different sources

Sources of Samples	No. of samples	No. of Isolates	*Bacillus* isolates
Soil	30	28	B1, B2, B3, B4, B5, B6, B7, B8, B9, B10, B11, B12, B13, B14, B15, B16, B17, B18, B19, B20, B21, B22, B23, B24, B25, B26, B27 and B28
Water	15	7	Bw2, Bw6, Bw7, Bw8, Bw9, Bw10 and Bw12
Meat	15	5	Bm2, Bm3, Bm4, Bm5 and Bm6
Total	60	40	

Table 2: Protein hydrolysis in Skim milk-peptone agar (at pH7.0 and pH8.0) cultured with *Bacillus* isolates and incubated for 24h. at 40°C.

Code number of isolates	Hydrolysis ratio(1)		Code number of isolates	Hydrolysis ratio		Code number of isolates	Hydrolysis ratio	
	pH 7	pH 8		pH 7	pH 8		pH 7	pH 8
B1	4	4	B5	1.3	1	B18	1.2	1
B20	3.5	3	B4	1.3	1	Bw7	1.2	1
B7	3	2.7	B12	1.3	1	Bw12	1.2	1
B3	2.4	2.7	Bm2	1.3	1	B2	1.2	1
B26	2	2.4	B21	1.2	1	B27	1.1	1
B15	2	2	B14	1.2	1	B10	1.1	1
B2	1.7	1.5	B13	1.2	1	Bw8	1.1	1
B11	1.7	1	Bm4	1.2	1	Bw9	1.1	1
B17	1.7	1	B28	1.2	1	Bm3	1.1	1
B16	1.6	1	B22	1.2	1	B6	1.1	1
B24	1.5	1	B23	1.2	1	Bw10	1.1	1
B8	1.5	1	Bm5	1.2	1			
B9	1.3	1	B25	1.2	1			
LSD Value:0.05	pH 7		0.729 *					
	pH 8		0.633 *					

(1) Diameter of clear zone/Colony diameter.

Table (3): Specific activities of protease produced by *Bacillus* isolates after 24h. incubation at 40°C in Peptone-casein broth (pH 8).

Code Number of isolates	Specific activity(U/mg protein)
B1	4.4
B20	3.7
B7	3.2
B3	3.0
B26	2.3
B1[2]	2.0
B15	1.8
LSD Value : 0.05	0.702 *

Table 4: Morphological and Biochemical characteristics of *Bacillus* B1 isolate.

Characteristics	*Bacillus licheniformis*
Cell shape	Rod
Spore shape	Ellipsoidal
Spore site	Central
Gram stain	+
Catalase	+
Motility	+
Voges-Proskauer	+
Starch hydrolysis	+
Protease production	+
Egg-yolk reaction	-
Nitrate reduction	+
Sodium chloride tolerance 7%	+
Growth at 50°C	+
Citrate utilization	+
Anaerobic growth	+
Gelatin hydrolysis	+
Carbohydrates fermentation	
Galactose	+
Glucose	+
Maltose	+
Sucrose	+

+: positive result, -: negative result.

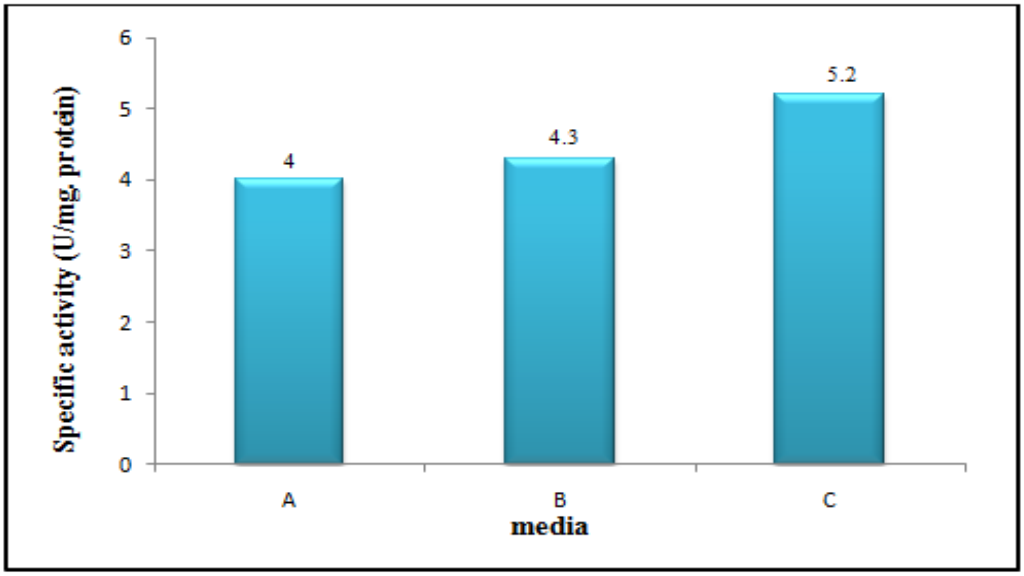

Figure 1: Protease production by *B. licheniformis* B1 cultured in different media incubated at 37˚C. for 24 hrs. at pH 8.0; A: Casein–peptone medium. B: Horikoshi medium. C: Casein-yeast extract medium. [LSD Value: 0.05 = 0.493]

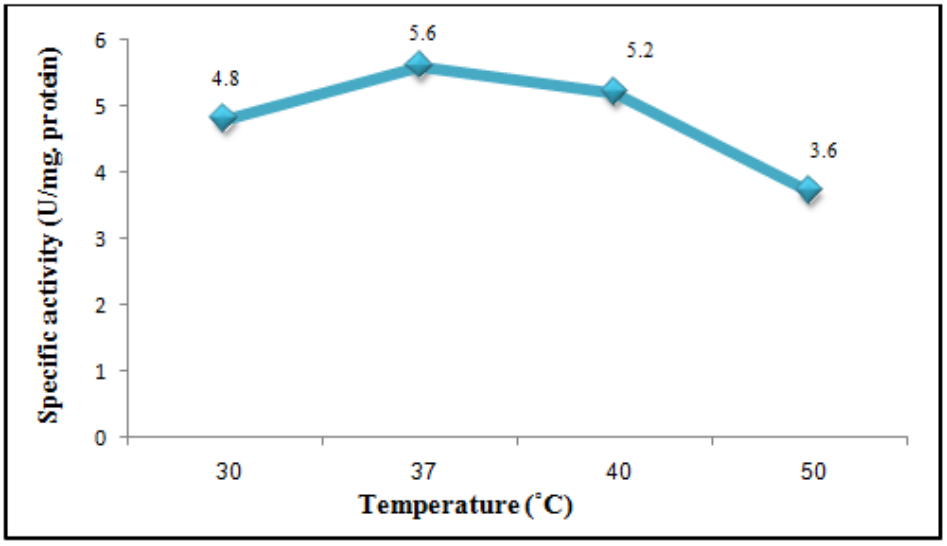

Figure 2: Protease production by *B. licheniformis* B1 cultured in casein-yeast extract medium pH 8.0 and incubated at different temperatures for 24 h.
[LSD Value: 0.05 = 1.02]

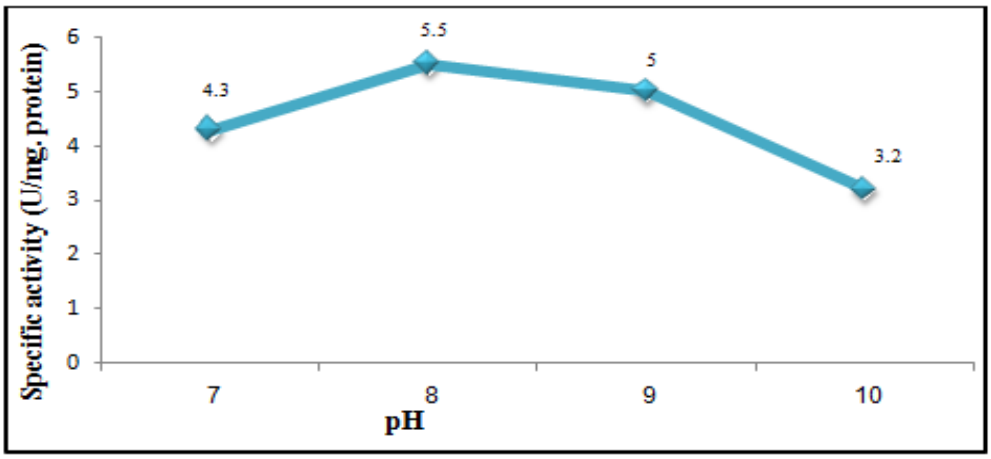

Figure 3: Protease production by *B. licheniformis* B1 cultured in casein-yeast extract medium prepared at different pHs and incubated at 37˚C. for 24h.
[LSD Value: 0.05 = 1.16]

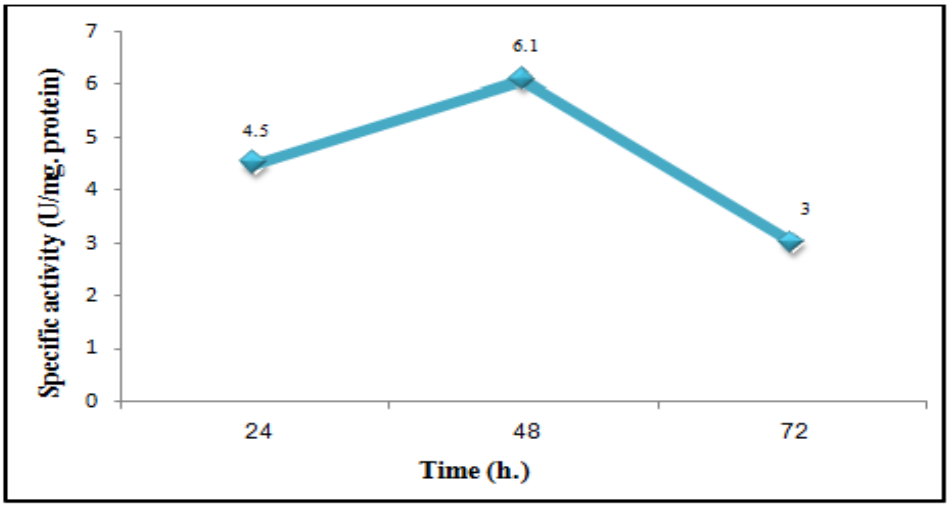

Figure 4: Protease production by *B. licheniformis* B1 cultured in casein-yeast extract medium prepared at pH 8.0 and incubated at 37°C for different times. [LSD Value: 0.05 = 1.55]

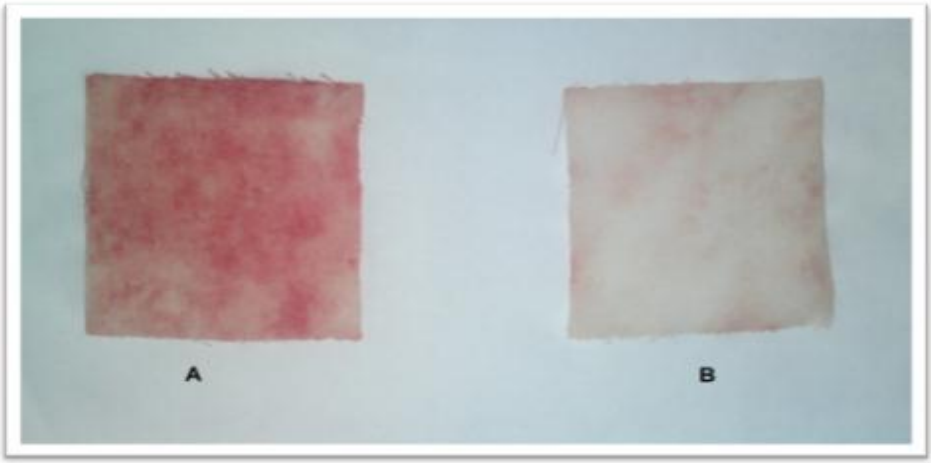

Figure (5): Removal of blood colors from cloth piece by crude protease of *B. licheniformis* B1. The blood-cotaining cloth piece was incubated with crude protease at 30°C for 30min. A, control (without enzyme); B, Sample treated with enzyme.

Figure (6): Removal of gelatin from X-ray films by crude protease of *B. licheniformis* B1. The X-ray films pieces were incubated with crude protease at 30°C. for 2h. A, control (without enzyme); B, Sample treated with enzyme.

References

1. Khan, M.A., Ahmad, N., Zafar, A.U., Nasir, I.A., Qadir, M.A. (2011) Isolation and screening of alkaline protease producing bacteria and physio-chemical characterization of the enzyme. Afr. J. Biotechnol. 10(33): 6203-6212.
2. Jon, S. (2008) Global Industry Analysts. www.theprofitdepot.com.
3. Deng, A., Wu, J., Zhang, Y., Zhang, G., Wen, T. (2010) Purification and characterization of a surfactant-stable high-alkaline protease from *Bacillus* sp. B001. Bioresource Technol. 101(18): 7100-7106.
4. Joo, H.S., Chang, C.S. (2005) Production of protease from a new alkalophilic*Bacillus sp.* I-312 grown on soybean meal: optimization and some properties. Proc. Biochem. 40: 1263-1270.
5. Kocher,G.S., Mishra, S. (2009) Immobilization of *Bacillus circulans* MTCC 7906 for enhanced production of alkaline protease under batch and packed bed fermentation conditions. Int. J. Microbiol. 7: 359-378.
6. Shumi, W.M., Hossain, T., Anwar, M.N. (2004) Proteolytic activity of a Bacterial isolate *Bacillus fastidiosus* den Dooren de Jong .JBS. 4: 370-374.
7. Logan, N. A., De Vos, P. (2009) Genus I. *Bacillus* Cohn 1872. p. 21-128. In: De Vos, P. (eds) Bergey's Manual of Systematic Bacteriology, 2nd edn, Vol 3. Springer, New York.
8. Sharma, J., Singh, A., Kumar, R., Mittal, A. (2006) Partial purification of an alkaline protease from a new strain of *AspergillusOryzae* AWT 20 and its enhanced stabilization in entrapped Ca-alginate beads. Int. J. Microbiol.2 (2).
9. Ramakrishna, D.P.N., Gopi, N.R., Rajagopal, S.V. (2010) Purification and properties of an extra cellular alkaline protease produced py*Bacillus Subtilis* (MTTC N0-10110). Int. J. Biotechnol. Biochem. 6(4): 493-504.
10. Anson, M.L. (1938) The estimation of pepsin, trypsin, papain and cathepsin with haemoglobin. J. Gen. Physiol. 20: 79-89.
11. Horikoshii, K. (1999) Extracellular enzymes isolation procedures for alkaline enzymes. In: Alkaliphiles.Kodensha Ltd. Tokyo.147.

12. Rao, K., Narasu, M.L. (2007) Alkaline protease from *Bacillus firmus* 7728. Afr. J. Biotechnol. 6 (21):2493-2496.
13. SAS .2004. SAS User's Guide :Statistics Version .7.0 , SAS Institute . Inc. Cary, NC. USA.
14. Slepecky, R.A., Hemphill, H.E. (2006) The genus Bacillus-nonmedical, P.530–562,.in: Dworkin, M. (eds) The Prokaryotes, A Handbook on the Biology of Bacteria:, Third Edition, Volume 4. Springer, New York.
15. Nunes, A.S., Martins, M.L.L. (2001) Isolation, properties, and kinetics of growth of a thermophilic*Bacillus*. Braz. J. Microbiol. 32:271–275.
16. Arulmani, M., Aparanjini, K., Vasanthi, K., Arumugam, P., Arivuchelvi, M., Kalaichelvan, P. T., (2007) Purification and partial characterization of serine protease from thermostablealkalophilic*Bacillus laterosporus*-AK1. World J. Microbiol. Biotechnol. 23:475–481.
17. Genckal, H., Tarib, C. (2006) Alkaline protease production from alkalophilic*Bacillus* sp. isolated from natural habitats. Enzyme and Microbial Technology 39:703–710.
18. Sakai, K., Yamanami, T. (2006) Thermotolerant*Bacillus licheniformis*TY7 produces optically active L-lactic acid from kitchen refuse under open condition. J. Biosci. Bioen. 102 (2): 132–134.
19. He, L., Chen, W., Liu, Y. (2006) Production and partial characterization of bacteriocin-like pepitdes by *Bacillus licheniformis* ZJU12. Microbiol. Res. 161: 321-326.
20. Boominadhan, U., Rajakumar, R., Sivakumaar, P. K. V., Joe, M. M. (2009). Optimization of protease enzyme production using *Bacillus* Sp. isolated from different wastes. Botany Res. Int. 2(2): 83-87.
21. Ghafoor, A., Hasnain, S. (2009) Production dynamics of *Bacillus subtilis* strain AG-1 and EAG-2, producing moderately alkaline proteases. Afr. J. Microbiol. Res. 3 (5): 258-263.
22. Uyar, F., Porsuk, I., Kizil, G., Yilmaz, E.I. (2011) Optimal conditions for production of extracellular protease from newly isolated *Bacillus cereus* strain CA15. Eur-Asia J. BioSci. 5: 1-9.
23. **Prescott**, L. M., Harley, J., Klein, D.A. (2005) Microbiology.(6th Ed.).Published by McGraw Hill. New York.
24. Martins, M. L., Teodoro, C.E. (2000) Culture condition for the production of thermostable amylase by *Bacillus* sp. Braz. J. Microbiol. 31(4): 982-302.
25. Nadeem, M., Qazi, J.I., Baig, S., Syed, Q. (2007) Studies on commercially important alkaline protease from *Bacillus licheniformis*N-2 isolated from decaying organic soil. Tur. J. Biochem. 32: 171-177.
26. Ray, M.K., Devi, K.U., kumar, G.S., Shivaji, S. (1992) Extracellular protease from yeast *Candida humicola*. Appl. Environ. Microbiol. 58:1918–1923.
27. Puri, S., Khalil, O., Gupta, R. (2002) Optimization of alkaline protease production from *Bacillus* sp. by response surface methodology. Curr. Microbiol. 44:286–90.
28. Ashgher, M., Javaid-Asad, M., Rahman, S.U., Legge, R.L. (2007) A thermostable α-amylase from a moderately thermophilic*Bacillus subtilis* strain for starch processing. J. Food Eng. 79: 950–955.

29. Mona, A., Esawy, W., Helmy, A., Samia, A., Yannick, C. (2007) Natural material role in production, activation and stabilization of alkaline protease produced from a new isolated *Geobacillus caldoxylosilyticus*. J. App. Sci. Res. 3(10): 106–109.
30. Sayem, S.M.A., Alam, M.J., Hoq, M.M. (2006) Effect of temperature, pH and metal ions on the activity and stability of alkaline protease from novel *Bacillus licheniformis* MZK03. Proc. Pakistan Acad. Sci. 43(4):257-262.
31. Mona, K., Goud, A. (2006) Optimization and purification of alkaline proteases produced by marine *Bacillus* sp. MIG newly isolated from eastern harbour of Alexandria. Polish J. Microbiol. 55(2):119–126.
32. Nguyen, T.T, Quyen, D. T. (2011) Overproduction of an extracellular protease from *Serratia* Sp. DT3 Just Using Soybean Powder. World J. Agric. Sci. 7 (1): 29-36.
33. Olajuyigbe, F. M, Ajele, J.O. (2011) Some properties of extracellular protease from *Bacillus licheniformis*Lbbl-11 isolatedfrom "iru", a traditionally fermented African Locust Bean Condiment. Global J. Biotechnol Biochem. 3 (1): 42-46.
34. Dodia, M.S, Bhimani, H.G., Rawal, C.M., Joshi, R.H., Singh, S.P. (2008) Salt dependent resistance against chemical denaturation of alkaline protease from a newly isolated halophilic Bacillus sp. Bioresour. Technol. 99: 6233-6227.
35. Nadeem, M., Qazi, J.I., Baig, S., Syed, Q. (2008) Effect of medium composition on commercially important alkaline protease production by *Bacillus licheniformis*N-2.Food Technol. Biotechnol. 46(4): 388- 394.
36. Gehan, M., Abou-Elela, G.M., Ibrahim, H.A.H., Hassan, S.W., Abd-Elnaby, H., El-Toukhy, N.M.K. (2011) Alkaline protease production by alkaliphilic marine bacteria isolated from Marsa-Matrouh(Egypt) with special emphasis on *Bacillus cereus* purified protease. Afr. J. Biotechnol. 10(22): 4631-4642.
37. Vishalakshi. N., Lingappa, K., Amena, S., Prabhakar, M., Dayanand, A. (2009) Production of alkaline protease from *Streptomicesgulbargensis* and its application in removal of blood stains. Indian J. Biotechnol. 8: 280-285.
38. Shankar, S. (2010) Stability of protease in organic solvents, detergents and denaturants.Ph.D. Thesis, University of Pune.
39. Vijayalakshmi, S., Venkatkumar, S. Thankamani, V. (2011) Screening of alkalophilicthermophilic protease isolated from *Bacillus* RV.B2.90 for Industrial applications. Res. Biotechnol. 2(3): 32-41.

Assessment of Radiological Status for the Destroyed Nuclear Fuel Fabrication Facility at AL-Tuwaitha Site

Dr. Yousif M. Zayir Al-Bakhat (Ph.D)*, Hussein J. Mugar,Qusay A. Abdulhadi, Nabeel H. Ameen, Fouzey H. Kitah, Mohammed Adel Jawad and Hassan M. Ali

Ministry of Science & Technology, Radiation & Nuclear Safety Directorate

*yousif_zayir@yahoo.com

Ph. 00964 7811332431

Abstract

The fuel fabrication facility (FFF) is one of the destroyed nuclear facilities in AL-Tuwaitha site that requires remediation and decommissioning. The characterization of activities of FFF had been conducted in 2013 using hand-held radiation detection instruments for the structures and the surface of FFF for contaminations. The exposure dose rates and laboratory measurement was conducted for forty nine soil samples that collected for activity measurements and analysis using gamma spectrometry technique of high purity germanium detector. The surveys and laboratory results indicated that the FFF was contaminated with uranium-238 and uranium-235 nuclides in excess of the IAEA limits for exemption from regulatory control, and indicating that the decommissioning operations for the FFF must be subjected to regulatory control and safety surveillance to ensure adequate protection of the operators, public and the environment during implementation of the decommissioning operations, according to ALARA (As Low As Reasonable Achievable) principle as recommended by International Atomic Energy Agency (IAEA).

Key words: Radiological characterization, Fuel fabrication facility, Iraqi decommissioning program (IDP), Radiological safety.

تقييم الحالة الاشعاعية لمنشاة صناعة الوقود النووي المدمرة في موقع التويثة

الخلاصة

منشاة صناعة الوقود النووي هي احدى المنشات النووية في موقع التويثة التي تتطلب تنظيفها وتفكيكها. اجريت عمليات التوصيف الاشعاعي لهذه المنشاة خلال عام 2013 باستخدام الاجهزة المحمولة للتلوث الاشعاعي و التعرض الاشعاعي للأبنية وارضية المنشأة وكذلك بواسطة اجهزة التحليل المختبرية حيث تم جمع(49) نموذج تربة وجرى قياس النشاط الاشعاعي للنماذج باستخدام منظومة تحليل اطياف كاما المتكون من كاشف الجرمانيوم عالي النقاوة. بينت نتائج التوصيف الاشعاعي ان الموقع ملوث بنظائر اليورانيوم-238 واليورانيوم-235 بمستويات تتجاوز معايير الاعفاء من السيطرة الرقابية والمعتمدة من قبل الوكالة الدولية للطاقة الذرية، وأن عمليات تنظيف وتصفية هذه المنشاة يجب ان تخضع للسيطرة الرقابية لضمان صحة وسلامة العاملين وعامة السكان والبيئة خلال تنفيذ عمليات التصفية و تقليل مستويات التلوث والتعرض الاشعاعي الى اقل قدر ممكن وحسب مبدا (ALARA)الموصى به من قبل الوكالة الدولية للطاقة الذرية .

الكلمات المفتاحية: التوصيف الاشعاعي، منشاة صناعة الوقود، برنامج التصفية العراقي، السلامة الاشعاعية.

Introduction

Fuel Fabrication Facility (FFF) is one of nuclear facilities located within Al-Tuwaitha nuclear site,GPS Coordinates (North= 33°11.462˝, East= 44°30.723˝) (Figures 1 and 2). It was designed to manufacture nuclear fuel (natural UO_2) with the requirements of nuclear technology in laboratory scale [1-3]. The FFF wasused to prepare nuclear fuel pins of maximum length (4.1 m) and to assembly fuel element of maximum length (4.5 m), which irradiated at Iraqi nuclear research reactor IRT 5000 kW for the purpose of radiochemistry research. The Fuel Fabrication Facility was established by Italy in 1980 at Al-Tuwaitha Nuclear Site of the previous Iraqi Atomic Energy Commission (IAEC). It was operated in 1981 and destroyed in 1991 in the second gulf war. Now, only steel skeleton remains and large piles of concrete, rubbles, soil, steel, unsafe structure and the surroundings area were contaminated with Uranium compounds such as (UO3, UO2) as a result of operation and the dispersion of uranium due to facility bombarding by coalitionforces. The FFF covered ground area of about 32000 $m^2$and consists of the constructions as shown in Figure 3 and 4.

Fig. 1.Location of (FFF) inside Al-Tuwaitha site.Fig. 2. Shows the current condition of FFF

The purpose of study was to assess the radiological activity to be used as a basis for evaluating the radiological impact risk due to decommissioning operations on the operators, public and the environment.

Materials and Methods:

Typical methods were used to determine the radiological condition of areas, equipments, and systems, for destroyed fuel fabrication facility in radiological characterization process.

Instrumentation

The instruments were selected for the external exposure dose rates and contaminations of the destroyed FFF were determined using different types of portable instruments types:

- Ludlum model (2241-2) with model 44-10 Sodium Iodide (NaI) 2"×2" Detectorfor measuring gamma dose rate in (µSv/hr), with sensitivity of approximately 900 count per minute (cpm) per (µR/hr) for Cs-137.

- Radeye-sx with100cm^2 scintillation probe model DP6BD for measuring (α, β, and γ) contaminationin unit (Bq/cm^2), a zinc sulfide (ZnS(Ag)) scintillation detector ,with gamma sensitivityapproximately 15-20 cpm/µR/hr for Cs-137.

Measurements:

Background Measurements:

The background measurements for dose rates and contaminations were done at 150 m far from North of the FFF at coordinate(N 33 12,072. E 44 30, 721), because this location was free from any contamination and had the same components (soil, steel, rubble, concrete, etc.).Grid (10 m x 10 m) was chosen to perform background measurement [4-6]. The results of radiological background measurements are shown in Table-1:

Table 1. Background measurements

Measurements ofthe destroyed Fuel Fabrication Facility (FFF)

The surface area of the facility was divided into 320 grids, each grid was divided to (10 m x10 m), initial point (0, 0) located at the left end of the entrance, y –axis represent the south of the facility, while X-axis represent the west. Number of grids on Y-axis is 16 grids while number of grids on X-axis was 20 grids. The dose rate measurements were done at 15 cm height above the ground levels, the average for each grid were determined for 20 number of measurements in (µSv/h), while the contamination measurements were done for measuring (α, β, and γ) contaminations at height 5 cm in Bq/cm^2 for 20 number of measurements at each grid and moved in a serpentine pattern to cover whole grid while walking at a speed that allows the investigator to detect the desired investigation level [7-10]. Figures (3, 4) show the contamination areas and construction of FFF.

Type of material	Contaminations (Bγ) Bq/cm^2 By RadEye SX with DP6BD scintillation (100cm^2) detector at height 5 cm above the ground surface			Dose rates µSv/h (γ) by Ludlum Sodium Iodide (NaI) 2"×2" Detector at height 15 cm above the ground surface		
	MIN.	MAX.	AVAR.±SD	MIN.	MAX.	AVAR..±SD
Concrete	0.090	0.140	0.108±0.013	0.046	0.063	0.057±0.004
Soil	0.090	0.150	0.128±0.019	0.063	0.081	0.070±0.006
Asphalt	0.090	0.140	0.113±0.014	0.049	0.058	0.053±0.002
Steel	0.090	0.140	0.102±0.014	0.045	0.059	0.051±0.004

SD= Standard deviation

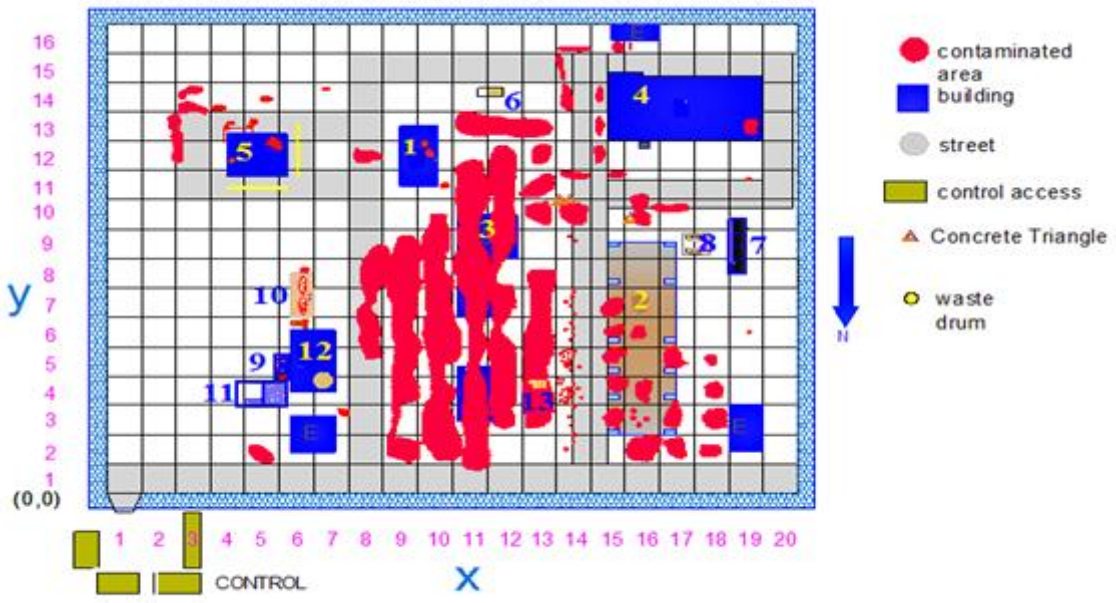

Fig 3: Ground Contamination area of FFF which is illustrated in red color.

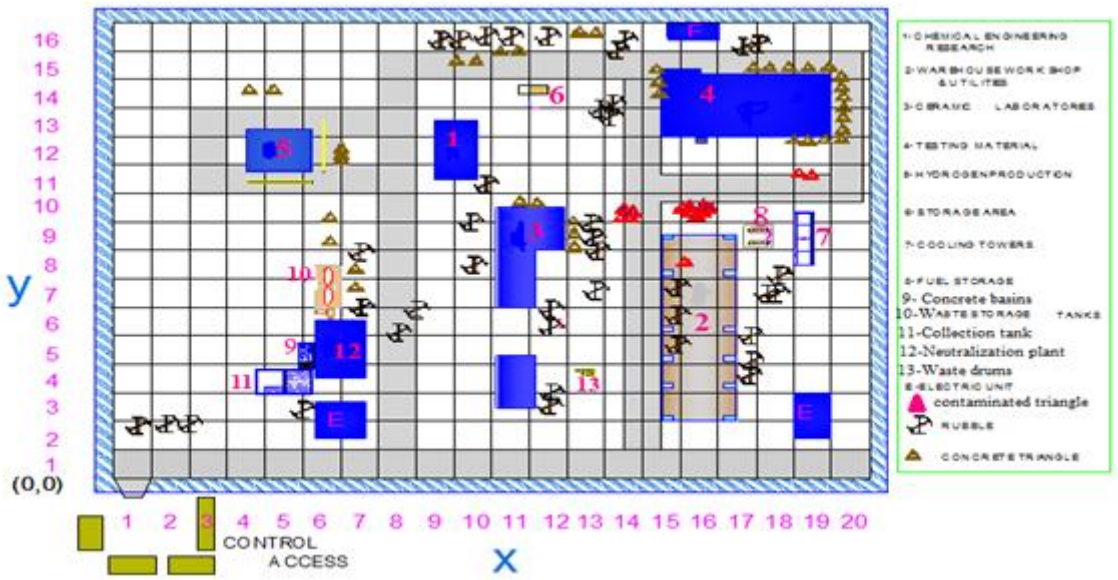

Fig. 4.The constructions and gridding of ground of (FFF).

Table 2. Measurement for dose rate and contaminations of FFF

No.	Measurement Location	Dose rate at 15cm by Ludlum µsv/h			Contamination measurements by radeyeBq/cm^2		
		Min.	Max.	Aver.±SD	Min.	Max.	Aver.±SD
1	Waste drums	0.236	1.867	0.702±0.352	3.700	54.710	29.300±17.708
2	Underground channels	0.043	0.372	0.056±0.084	0.090	6.030	0.510±1.534
3	Neutralization concrete basins	0.057	0.688	0.212±0.198	0.120	62.300	4.480±3.511
4	Radioactive liquid waste tank	4.605	30.000	16.681±3.667	0.150	492.300	89.380±49.5
5	Technological Hall	0.045	0.247	0.077±0.051	0.130	10.500	0.510±1.567
6	Ceramic laboratories	0.057	4.053	0.314±0.473	0.120	80.800	8.100±5.523
7	Hydrogen Production Building	0.065	0.154	0.094±0.091	0.110	1.480	0.230±0.150
8	Ware house, Work Shop and Utilities Building	0.052	6.492	0.454±0.269	0.110	420.000	32.100±28.834
9	Hall for Testing Material	0.051	0.062	0.058±0.018	0.090	9.130	0.240±0.328
10	concretes triangle	0.098	1.534	0.573±0.310	0.110	145.000	29.400±24.683
11	Chemical waste treatment and neutralization plant	0.057	0.082	0.062±0.011	0.100	0.180	0.140±0.021
12	Surrounding areas	0.061	4.543	0.213±0.475	0.360	84.600	5.300±9.538
13	Electric units	0.053	0.091	0.062±0.008	0.120	0.180	0.140±0.015
14	Cooling tower	0.052	0.069	0.058±0.005	0.110	0.140	0.120±0.012
15	Collection tank	0.062	0.088	0.068±0.006	0.120	0.350	0.190±0.025

Laboratory measurements

Forty-nine surface soil samples (45 from inside the FFF and 4 samples from outside the FFF as background) were collected from different location of the facility to cover approximately the whole area of the facility and focused on the elevated areas that have a potential contamination according to survey measurements. The samples collected at depth of 5 centimeters using hand augerand there are only three soil samples were taken at depth 20 -30 cm, each soil sample was packed into its own secure bag to prevent cross contamination and sent to the laboratory for measurements. Soil samples were crushed by grinding machine and sieved through a 1 mm mesh sieve, and then dried in an oven at 80 – 100 ^{0}C for 5 h. One kilogram was packed in marinelli beaker geometry, closed and tightly sealed using par film and store about one month to allow U-

238 and Th-232 decay series to reach radioactive equilibrium with it short live progeny. Gamma spectrometer (Canberra) system was used to measurement and analyze samples, which consists of a detector, preamplifier and pulse-height analyzer (DSA 2000), lead shield, using vertical high purity germanium (HpGe) detector of efficiency 40 %, and resolution (2.0 keV). Based on the measurement of 1.332 MeV gamma ray photo peak of Co-60 source and Multichannel analyzer (MCA) with 8192 channel was used, both high voltage supply and amplifier device are compact in one unit (DSA 2000), A detector shield with a cavity adequate to accommodate large samples. Shield has walls 10 cm lead, thick lined inside with graded absorber of Cd ~ 1.6 mm Cu ~ 0.4 mm [5-7],calibration and efficiency of the system were carried out using multi–gamma ray standard source (MGS-5, canberra) of Marinelli beaker geometry and the time of measurements about 1 h. A library of radionuclides contained the energy of the characteristic gamma emissions of each nuclide was analyzed and their corresponding emission probabilities were built from the data supplied in the software (Genie-2000) [11-14] .The activity concentrations of radionuclides in soil sample are given in table (3), where Figure (5) showed the location of these samples. The specific activity in terms of the activity concentration is defined as the activity per unit mass of the sample. The specific activity of individual radionuclides in soil samples is given by the following equation [7]:

$$A = \frac{N}{\varepsilon_f P_\gamma t_s m K}$$

Where *N* = the corrected net peak area of the corresponding full-energy peak

N = NS - NB

NS = the net peak area in the sample spectrum

NB = the corresponding net peak area in the background spectrum

f = the efficiency at photo peak energy

ts= the live time of the sample spectrum collection in seconds

m = the mass (kg) of the measured sample

P= the gamma-ray emission probability corresponding to the peak energy

K = the correction factor

Table 3. Activity concentrations of radionuclides in soil samples (Bq/Kg). BDL; Below Detection Limit.

No.	Code of sample	No. of grid	Radionuclide concentrations (Bq/Kg)					
			U-238		U-235	Th-232	K-40	Cs-137
			Bi-214	Pa-234M				
1	IFS-1	1-2	12.8±0.9	BDL	BDL	12.9±1.1	475.5±12	BDL
2	IFS-2	1-10	13±0.8	BDL	BDL	14.9±1.1	299.7±17.1	2.5±0.3
3	IFS-3	19-16	16.9±0.89	BDL	BDL	11.8±0.7	237.4±14.5	1.7±0.2
4	IFS-4	2-2	14.8±0.95	BDL	BDL	7±1.6	392±14.5	3.17±0.33
5	IFS-5	2-8	18.4±1.14	BDL	BDL	16.1±1	334.5±20.1	3.2±0.42
6	IFS-6	2-16	12.5±1.3	BDL	BDL	8.4±1.2	453±15	BDL
7	IFS-7	3-12	7.5±0.9	6211.6±249.6	149±8.9	8.6±1.3	258±11.3	7.3±0.85
8	IFS-8	3-13	53±9.6	975758±19167	21203±365.6	BDL	379.6±44.4	BDL
9	IFS-9	4-14	11.7±1.8	18952±500.5	404.4±16.9	13.8±2.8	281±10.5	10.2±1.2
10	IFS-10	3-10	16.6±1.3	BDL	BDL	15.3±1.7	312±26.7	BDL
11	IFS-11	3-5	9.1±1	BDL	BDL	13.5±1.8	346±11	3.2±0.5
12	IFS-12	4-3	14.1±1.3	BDL	BDL	9.9±1.5	259.4±21	2.4±0.5
13	IFS-13	4-7	11.5±1.2	BDL	BDL	11±1.5	268.9±20.9	3.9±0.5
14	IFS-14	4-13	9.4±1.2	11942±396.9	290.4±11.4	12.3±1.6	270.2±20.4	4.3±0.6
15	IFS-16	5-13	17.4±2.5	94525±2066.1	2153.5±47.1	BDL	335±11	BDL
16	IFS-17	11-7	60±11.2	749005±14634.	15592±266.1	BDL	363.6±33.7	BDL
17	IFS-18	14-5	26±2.5	153174±3181.1	3656±71.7	BDL	253.4±22.5	BDL
18	IFS-19	17-3	29±3.4	224630±4495.5	4161±50.5	BDL	325±10.6	BDL
19	IFS-20	12-13	78±14.7	1125495±2181	16820±288.9	BDL	264±26.9	BDL
20	IFS-21	11-10	36±18.7	377785±7454.2	6744±119.4	14.9±5	124±18.9	BDL
21	IFS-22	10-7	62±12.9	539612±10755	13083±232.5	BDL	332±35.7	BDL

22	IFS-23	12-10	42±19.2	342493±6868.5	8179±147.9	BDL	283.6±28.7	BDL
23	IFS-24	20-11	11±0.85	BDL	BDL	14.9±1.1	316.±12.1	3.4±0.3
24	IFS-25	20.2	14±0.8	BDL	BDL	15.9±1.1	273.7±17.1	BDL
25	Core 5-2	5-2 at depth 20cm	17±1.8	135.7±60.2	BDL	21.9±2.5	440±32.4	BDL
26	Surface 5-2	5-2	13.3±1.7	10820.6±354.2	209±11.8	15±2.3	290.2±25.1	5.7±0.9
27	Core 8-6	8-6 at depth 20 cm	47.4±29.4	BDL	BDL	12±2.5	246±29.3	BDL
28	FFFS 9-2	9-2	25.1±2	8608.6±267.1	87.8±8.5	15.7±2.2	356.6±27.6	4.4±0.8
29	FFFS 9-6	9-6	14.6±1.4	12176.5±413.9	226.9±8.5	17.1±2.1	331.2±25	2.2±0.6
30	FFFS 9-14	9-14	16.3±1.1	BDL	BDL	14.2±1.4	328.5±21.1	0.96±0.3
31	FFFS 11-13	11-13	42.7±17	193956±4517	4367±1.9	BDL	75.9±25.4	BDL
32	FFFS 13-7	13-7	18.3±1.4	4273.1±210.3	93.6±11	16.3±3.2	287.3±24.7	5±1.2
33	FFFS 13-13	13-13	21.9±1.8	66290±1022.7	1482.2±39.2	15.8±2.2	333.6±22.7	BDL
34	FFFS 14-3	14-3	19.8±1.6	5215±220.8	92±7.4	18.2±2.5	287.2±23.1	3.4±0.6
35	FFFS 15-6	15-6	38±19.1	201993±913.1	4061.5±83	BDL	241.7±18.4	BDL
36	FFFS 15-5	15-5	40±23.3	286542.5±3778	5466.3±107	BDL	404.6±34.8	BDL
37	FFFS 15-16	15-16	25.6±2.2	17834.6±459.7	385±15.7	21.2±2.5	495±24.6	15±1.3
38	FFFS 16-2	16-2	18.9±1.9	31428±637.1	559±137	21.8±2.8	339.3±24.7	7.1±1
39	FFFS 16-	16-11	20±1.7	5597.4±240.9	123.6±8.9	14.4±2.6	343.6±26.6	BDL

	11							
40	FFFS 18-4	18-4	5.2±1.4	2606.3±155.4	55.7±4	10.6±1.7	295.6±23.9	3.2±0.6
41	FFFS 18-10	18-10	15.6±1.4	1021±91.9	BDL	11.8±1.6	317.2±24	7.9±0.8
42	FFF 19-13	19-13	15.6±1.5	6908.4±292.6	141.9±6.3	11.9±1.7	203.8±19.4	12.9±1
43	Surface 18-3	18-3	9.6±1.2	16901.4±491.4	299±11.8	8.7±1.5	218.8±17.6	BDL
44	Core 18-3	18-3 at depth 20 cm	8.9±0.8	126.4±35.9	BDL	8.1±0.8	179.4±14.5	BDL
45	bFFFS	B.G	16.3±1.2	BDL	BDL	12.1±0.9	327.3±22.3	3.2±0.4
46	bFFFS-1	B.G	21±3.7	BDL	BDL	16±4.7	478±65	4.1±1.8
47	bFFFS-2	B.G	14±2.1	BDL	BDL	10.4±2.4	439±47	2.5±0.7
48	bFFFS-3	B.G	13.7±1.9	BDL	BDL	14.1±1.2	385±53.5	4.2±0.9
49	BT	Storage tank	86±19.7	2233061±5981	28077.6±418	BDL	351±47.5	BDL

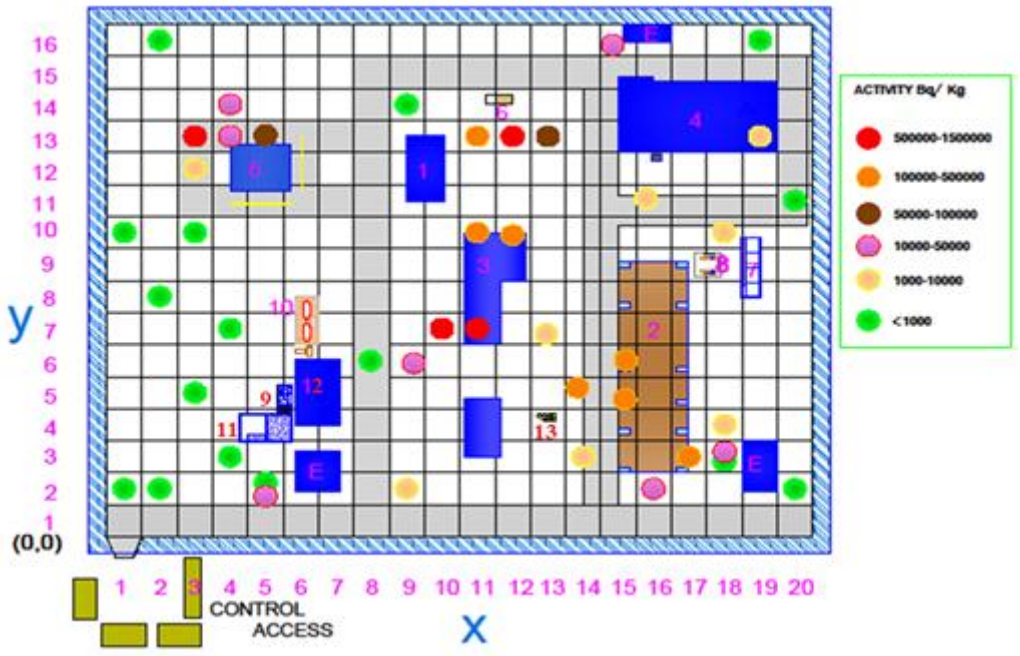

Fig. 5. Represents the soil samples location and the colors represent range of activities.

Results and Discussions

According to the field measurement and laboratory analysis, the FFF was contaminated with natural uranium with different level of activities. According to sample analysis, the maximum activity concentrations of surface soil sample was 1.125 MBq/Kg in grid 12-13 that was taken underneath the rubbles, while the dose rates and contaminations were 4.500μSv/h, 21.630 Bq/cm^2,respectively in the same grid, which were measured without removing the scrape and rubbles that can be considering as shielding for minimizing the exposure dose rates and contaminations also we found that the maximum dose rates, contaminations, and activity concentrations were 30.000 μSv/hr, 492.300 Bq/cm^2 , 2.233 MBq/Kg, respectively. In waste storage tank that located at depth -5 m of the FFF, the measurements were conducted directly without attenuation. The radiological survey and laboratory measurements and assessments, indicated that the FFF was contaminated with uranium-238 and uranium-235 nuclides in excess of the IAEA limits for exemption from regulatory control [4,9,10]. The ranges of activity concentrations of Cs-137 (0.96±0.3 ↔ 15±1.3), which considered as a background compared with the (IAEA) safety guide level was 100**Bq/Kg** [4]. The standard deviation of some readings were relatively high and that because high ranges in readings (minimum and maximum in same grid are high) and this variation in readings lead to high in standard deviation value. Radioactive waste that will be generated by the decommissioning operations are within low level waste (LLW) [13]. Therefore, the decommissioning operations for the FFF must be subjected to regulatory control and safety requirements to ensure adequate protection of the operators, environmental and public during the dismantling and decontamination operations, according to ALARA (As Low As Reasonable Achievable) principle as recommended by International Atomic Energy Agency (IAEA) [8, 12-14].

References

1. Abdulhadi, Q.A., AL-Bakhat, Y.M.Z. (2013) Preliminary Decommissioning Plan (DP) OF THE DESTROYED FUEL FABRICATION FACILITY (FFF), Ministry of Science and Technology, Baghdad, Revision 1.0 Submitted to IAEA.
2. IAEA. (2005) Standard format and content for safety related decommissioning document, safety series No. 45, IAEA, Vienna.
3. IAEA (2006) Decommissioning of Facilities Using Radioactive Material, Safety Standards Series No. WS-R- 5, IAEA, Vienna.
4. IAEA. (2004) Application of the concepts of exclusion, exemption and clearance, Safety Guide No.RS-G-1.7, IAEA, Vienna.
5. IAEA. (1998) characterization of radioactivity contaminated sites for remediation purpose, IAEA-TECDOC-1017, IAEA, Vienna.
6. IAEA (1998) radiological characterization of shutdown nuclear reactors for decommissioning purposes, T.R series No. 389, IAEA, Vienna.
7. IAEA. (1989) measurement of radionuclides in food and the environmental', a guide book, T.R. series No. 295, IAEA, Vienna.
8. IAEA. (1996) International Basic Safety Standards for Protection against Ionizing Radiation and for the Safety of Radiation Sources, Safety Series No. 115, IAEA, Vienna.

9. IAEA. (2006) Release of Site from Regulatory Control on Termination of Practices Safety Guide, WS-G- 5.1, IAEA, Vienna.
10. IAEA. (2005) Derivation of Activity Concentration Values for Exclusion, Exemption and Clearance, Safety Standards Series No. 44, IAEA, Vienna.
11. U.S.A, Laboratory Procedure Manual for the Environment Survey Program -ORIS (OAK RIDGE ISTITUTE FOR SCIENCE AND EDUCATION) U.S.A, 2007.
12. ICRP. (2000) protection of the public in situations of prolonged radiation exposure, ICRP publication 82; Ann, ICRP 29(1-2).
13. IAEA. (2006) Management of Problematic Waste and Material Generated During the Decommissioning of Nuclear Facilities, Technical Reports Series No. 441, IAEA, Vienna.
14. IAEA. (2007) Strategy and Methodology for Radioactive Waste Characterization, IAEA-TECDOC-1537, IAEA, Vienna.

Environmental Pollution in five floors (5^{th} to 9^{th}) Resulting From the use of Depleted Uranium Weaponry in the AL-Tahreer Tower Building

Nabeel hashim Ameen, Mazen Abbas Al-ghirrawy, Hamza Hadi Kadhim

Ministry of science and Technology

Ph. 00964 7811332431

ABSTRACT

The goals of this study include measuring the increase in radioactivity and removal the contamination regions to protect the population and the environment resulting from bombing the AL-Tahreer Tower Building (the Turkish restaurant previously) by the depleted uranium bullets through direct measurement and sampling of soil from five floors (5^{th},6^{th},7^{th},8^{th},and 9^{th}) of the building, which contains fourteen floors in addition to basement by using different types of portable monitoring equipments.

The results of radiological surveys by using the portable monitor (CAB) indicated the presence of contaminated soil reached to 55 c/sec, and small particles of depleted uranium shells has very high levels of contamination reached to 70 c /sec ,while the background level is (0.5c/sec) ,and the higher exposure rates is 55 µR/hr when the portable monitor (Ludlum) put on the contaminated regions approximately on distance 0.5 cm), where the natural background level is 9 µR/hr in the floors of the building.

The radiological analyses of the collected soil samples were done in the laboratory of the center of Radiological Researches in the Ministry of sciences and Technology by using gamma spectrometry (which contains High- purity Germanium Detector) with a efficiency of 40% and resolution 2 keV for Energy, 1.33Mev, collection, preparations and tests of soil samples were all done according to IAEA.The laboratory results indicated the presence of high concentrations of the isotopes Th-234 (1550.1) Bq/kg, and Pa-234m (1394.8) in the soil samples taken from the floors while the concentrations of Th-234 and Pa-234m in natural background levels are (nearly 40, nil) Bq/Kg respectively which is a clear indication of the presence of high concentrations an isotope of uranium - 238 as they are supposed to be in equilibrium radiation.

Keywords: radioactivity, AL-Tahreer Tower Building, contamination.

الخلاصة

إن خطة البحث شملت توصيف النشاط الإشعاعي لبناية برج التحرير(المطعم التركي سابقا) من خلال إجراء مسح إشعاعي لخمسة طوابق من البناية هي (الخامس ، السادس،السابع،الثامن،التاسع) والمتكونة من أربعة عشرا طابقا إضافة إلى السرداب وباستخدام أجهزة الكشف الإشعاعي المحمولة لغرض معرفة الزيادة الحاصلة في مستويات التعرض والتلوث الإشعاعي الناتجة من قصف بناية برج التحرير بإطلاقات اليورانيوم المستنفذ ،أظهرت نتائج المسوحات الإشعاعية التي أجريت باستخدام جهاز قياس معدل التلوث الإشعاعي CAB وجود تربة ملوثة يصل مستوى التلوث إلى 55 c/sec بالإضافة إلى وجود شظايا من إطلاقات اليورانيوم المستنفذ ذات مستويات تلوث عالية تصل إلى70 c/sec مقارنةً بمعدل الخلفية الإشعاعية (0.5 c/sec)، أما قراءات معدل الجرعة الإشعاعية للمناطق الملوثة باستخدام جهاز Ludlum فكانت 55 µR/hr عند وضع الكاشف على مسافة 0.5 cm تقريباً أما على مسافة 1 m فكانت 9 µR/hrوهي ضمن معدل الخلفية الإشعاعية الطبيعية.

كما وأخذت نماذج التربة وفق المعايير والمواصفات المعتمدة عالميا لهذا النوع من قياسات النشاط الإشعاعي،وتم قياسها باستخدام منظومة تحليل أطياف كاما والتي تتألف من عداد الجرمانيوم عالي النقاوة ذو كفاءة 40% وقدرة فصل 2 keV للطاقة 1.33 MeV،أظهرت نتائج الفحوصات المختبرية لنماذج التربة المأخوذة من مناطق قريبة من بناية برج التحرير والتي تعتبر كخلفية إشعاعية وجود نظير Th-234بنشاط إشعاعي قدره 40 Bq/kg وعدم وجود نشاط إشعاعي محسوس لنظير Pa-234m بينما أشارت نتائج نماذج التربة المأخوذة من طوابق البناية إلى وجود نشاط إشعاعي عالي لنظيري Th-234 و Pa-234m تصل إلى 1550.1 Bq/Kg و Bq/Kg1394.8 على التوالي والذي يعتبر مؤشر واضح على وجود نشاط إشعاعي عالي لنظير اليورانيوم- 238 لأنهما من المفروض أن يكونا في حالة توازن إشعاعي. وإن الهدف الأساسي من هذا البحث هو تقييم و معالجة التلوث الإشعاعي الناتج من قصف بناية برج التحرير بإطلاقات اليورانيوم المستنفذ لحماية السكان والبيئة من الآثار الضارة للأشعة المؤينة.

الكلمات المفتاحية: النشاط الاشعاعي، بناية برج التحرير، التلوث الاشعاعي.

INTRODUCTION

Uranium is found in trace amounts in all rocks and soil, in water and air, and in materials made from natural substances. It is a reactive metal, and, therefore, it is not present as free uranium in the environment. In addition to the uranium naturally found in minerals, the uranium metal and compounds produced by industrial activities can also be released back to the environment. Uranium can combine with other elements in the environment to form uranium compounds. The solubility of these uranium compounds varies greatly. Uranium in the environment is mainly found as a uranium oxide, typically as UO_2, which is an anoxic insoluble compound found in minerals and sometimes as UO_3, a moderately soluble compound found in surface waters. Soluble uranium compounds can combine with other chemical elements and compounds in the environment to form other uranium compounds. The chemical form of the uranium compounds determines how easily the compound can move through the environment, as well as how toxic it might be. Some forms of uranium oxides are very inert and may stay in the soil for thousands of years without moving downward into groundwater. The average concentration of natural uranium in soil is about 2 parts per million, which is equivalent to 2 grams of uranium in 1000 kg of soil [1].

DEPLETED URANIUM

Uranium is a radioactive chemical element in the periodic table, and is symbolized by the letter U. Atomic number is 92,and during the preparation of spent fuel for nuclear reactors ,processing and enrichment of Uranium is done to concentrate U-235 isotopes among other Uranium isotopes (U-230,U-234,U-238,U-235).the content ratios of these isotopes in the natural metal are 0.002% ,0.0058%,and 99.28% ,0.71% respectively [2] .Depleted Uranium (DU) is the highly toxic and radioactive byproduct of the Uranium enrichment process ,it is so called (Depleted)

because the content of the fissionable U-235 isotope is reduced from 0.7% to 0.2% during the enrichment process. The depleted Uranium is roughly 60% as radioactive as naturally occurring uranium metal, The weapons that enter the depleted uranium in the manufacture of multiple terms in the form of alloy consisting of (99.27%) uranium Depleted and (0.75%), titanium (TI-TI9V), and other types consisting of (98%) uranium depleted (2%) Molbydiom (Mo). Different sizes and dimensions of missiles depending on the uses and the type of weapon, of radioactive depleted uranium,the effectiveness of alpha particles in depleted uranium, less than normal by about 43 % [3].

Depleted uranium (DU) emits ionizing radiation and most of this radiation alpha particles and less beta and neither are moving a long distance in the tissue and therefore, the important impact happen by entering the body (breathing, eating ,or contamination of open wounds)[4].

DESCRIPTION OF THE BUILDING

The building located in the eastern door in front of the Tahreer Monument - the center of Baghdad, near the Tigris river to the west and surround with the shops and buildings of a commercial nature. The building consists of fourteen floor besides the basement, the area of each floor are approximately 640 m^2, the climbing to the floors building by the stairs that are on the right and left, and the Tahreer building contains in all floors on elevators and bathrooms which are currently unfavorable for use. Most floors in the building in the year 2003 exposed to the barrage, which led to damages in the structure of the building in some locations, and during the initial radiological survey by using radiation detection equipments, the team found; radioactive contamination in many floors resulting from direct hits with depleted uranium projectiles and the spread of radioactive contamination in the ground and walls and roofs of the building.

METHODOLOGY AND INSTRUMENTATION

1 – Determination of the background radiation:

The background was determined by measurement the exposure dose rate and contamination level around Tahreer Tower building .External exposure dose rates was performed using portable monitor Ludlum for gamma & beta, and the contamination rate was performed using portable monitor CAB for Alpha & Beta.

The level of contamination was determined by measuring the concentration of the potential radionuclide in the soil using gamma spectrometry techniques for the ground contamination of selected area surrounding Tahreer Tower building samples taken at depth of (5-10) cm [5].

2- Field work and portable instruments:

The exposure rates measurements were guided by using the portable scintillation counter type Ludlum (model 2241-2 survey meter Sweetwater Texaco, unit of measurement in µR/hr to R/hr) was used to measure Beta &Gamma absorbed dose rates in air, the counter consists of thallium - activated sodium iodide NaI(TI) crystal ,the instrument was calibrated using a Cs-137 standard source supplied by the manufacturer. The contamination rates measurements and the selection of the soil samples locations were guiding by using the portable rate meter type CAB (model- 18351 probe model SAB 70, Canberra, for measuring Alpha & Beta in cps). The instrument is held close to the surface, moved systematically that is sufficiently low to allow detection of changes in the radiation field.

The strategy of radiological survey was done through dividing the floors into grid boxes according to recommendations of

the IAEA and by selecting the front wall to the point of entry and give it the name (W1) and identify the rest of the walls counter-clockwise (W2,W3,W4) and apply this method on the ground(G) and ceiling(C), so the floors approximately divided into 44 grid boxes of (4.5 x 1.5) m^2 for walls , 200 grid boxes of (3 x 1) m^2 for ground ,and 20 grid boxes of (20 x 1.5) m^2 for ceiling, in each grid box ,measurements are taken at location near the center of the grid box as much as possible [6] .

3- Laboratory work:

The radiological analyses of the collected soil samples were done in the laboratory of the center of Radiological Researches in the Ministry of sciences and Technology by using Gamma spectrometry which contains High-Purity Germanium (HPGe) detector with efficiency of (40%) and resolution 2 keV at 1.33 Mev gamma ray photo peak of ^{60}Co source , the data are collected using digital spectrum analyzer (DSA-2000) furthermore the analysis of each measured gamma ray spectrum was conducted by dedicated software program (Genie-2000,USA) ,Marinelli beaker geometry is used for soil sample measurements ,calibration and efficiency of the system was carried out using multi–gamma ray standard source (MGS-5,Canberra) of Marinelli Beaker geometry . All sampling activities were recorded in the site and included sample specific information such as date, time of sampling, sample location and sample number. The collected soil samples were dried at room temperature for 10 days, the soil samples were grained by using 0.9 mm sieve [7] sample of a weight between (0.5-0.8) kg by using the electrical balance (Toledo with range 0.1-15 kg) was taken and contained in clean Marinelli Beaker, those Marinelli Beaker were placed in Gamma spectrometry for 3600 seconds for each sample. Activity in soil samples was reported on a dry weight basis in (Bq/kg).

RESULTS AND DISCUSSION

More than 50 exposure reading around the building indicated ,the natural exposure rate is **9** µR/hr& contamination rates is **0.5** cps .Firstly the portable survey meter (CAB-cps) was used to detection the contamination areas in the building, because the high sensitivity of portable contamination survey instruments comparing with exposure survey instruments. Figures (1, 2, 3, 4, and 5) show the results of the contamination rates measurements before decontamination processes in the floors (5^{th}, 6th, 7th, 8th, and 9^{th}).

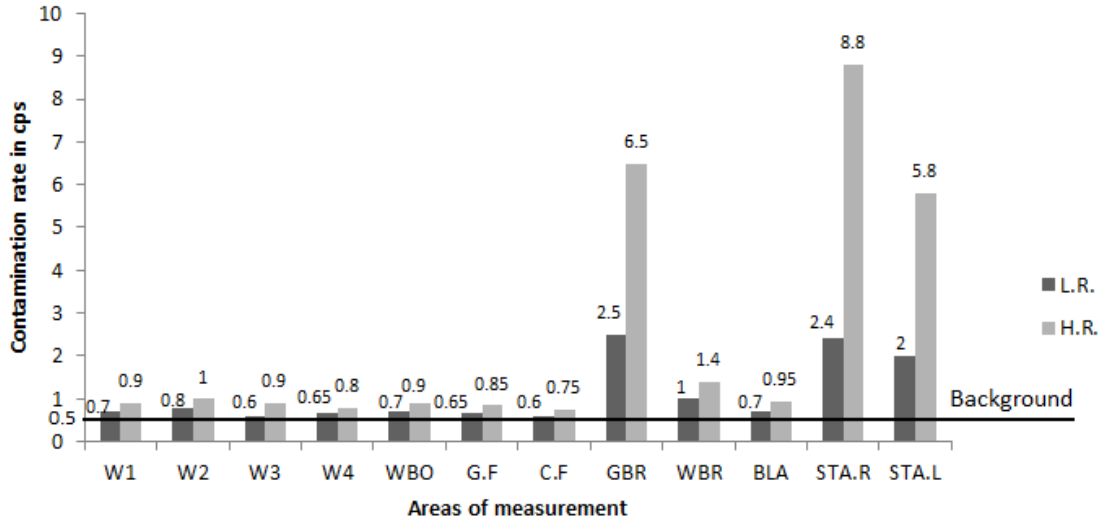

Figure (1) contamination rate in floor 5 before processes decontamination

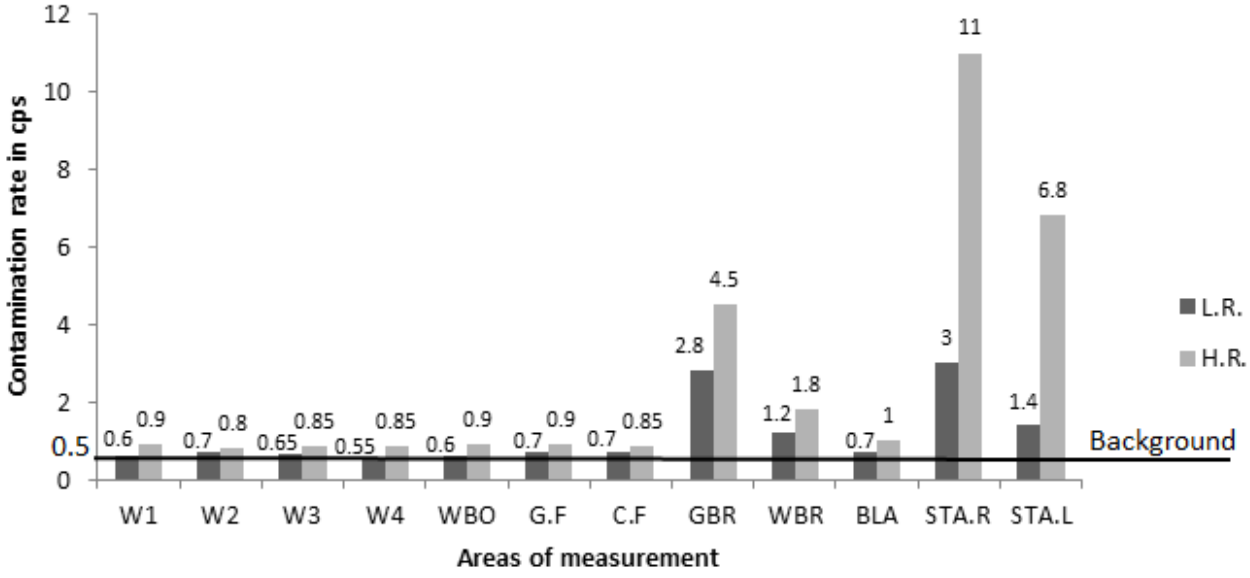

Figure (2) contamination rate in floor 6 before processes decontamination

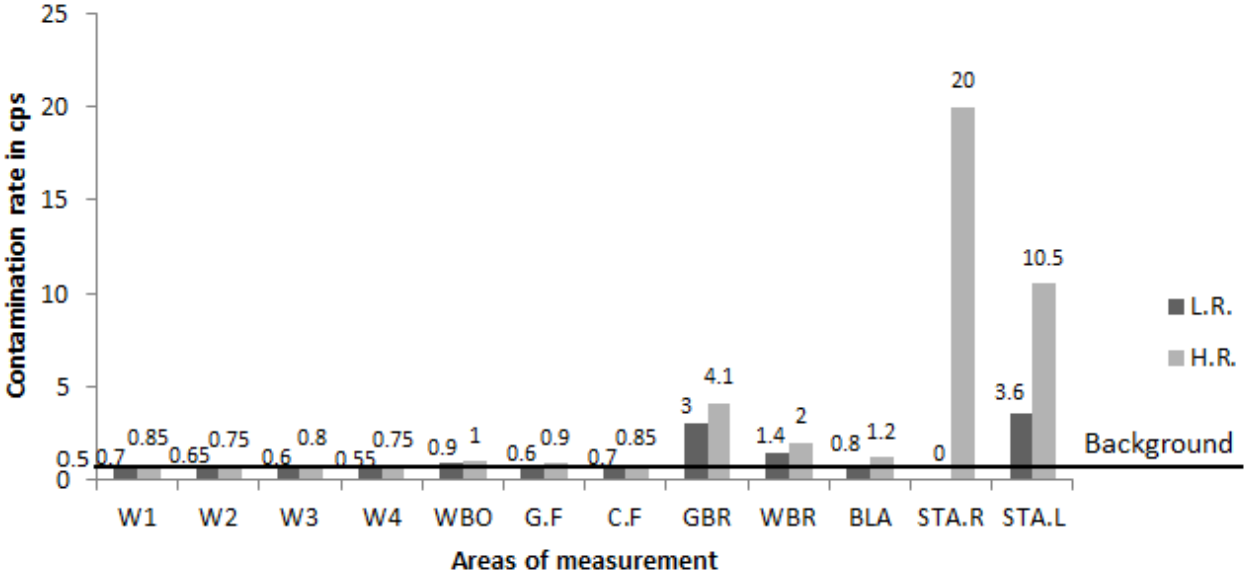

Figure (3) contamination rate in floor 7 before processes decontamination

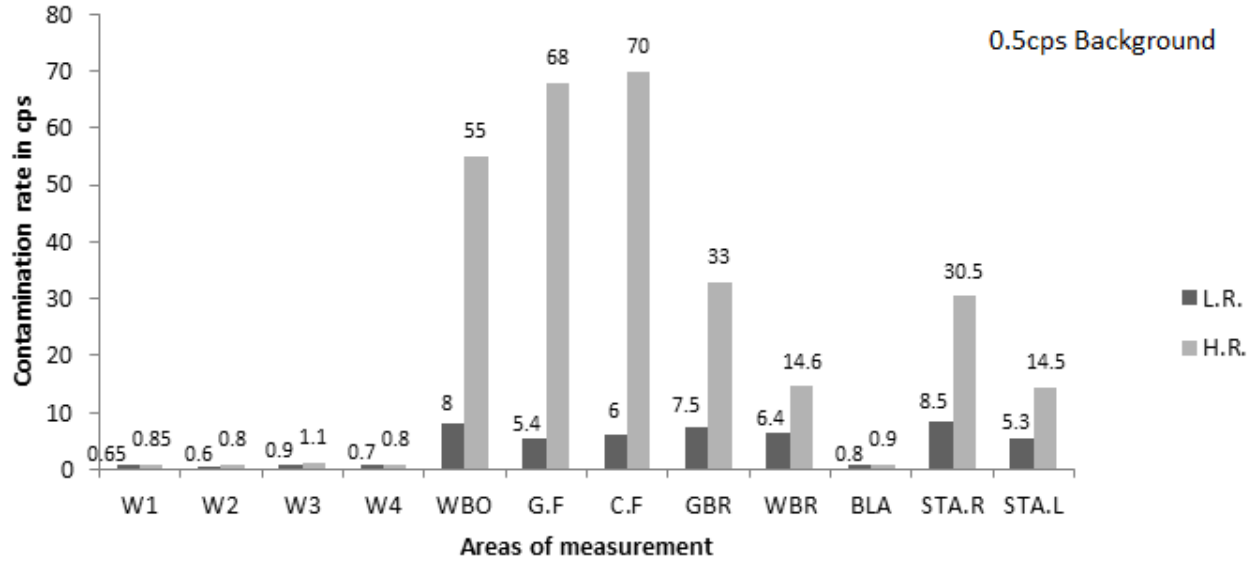

Figure (4) contamination rate in floor 8 before processes decontamination

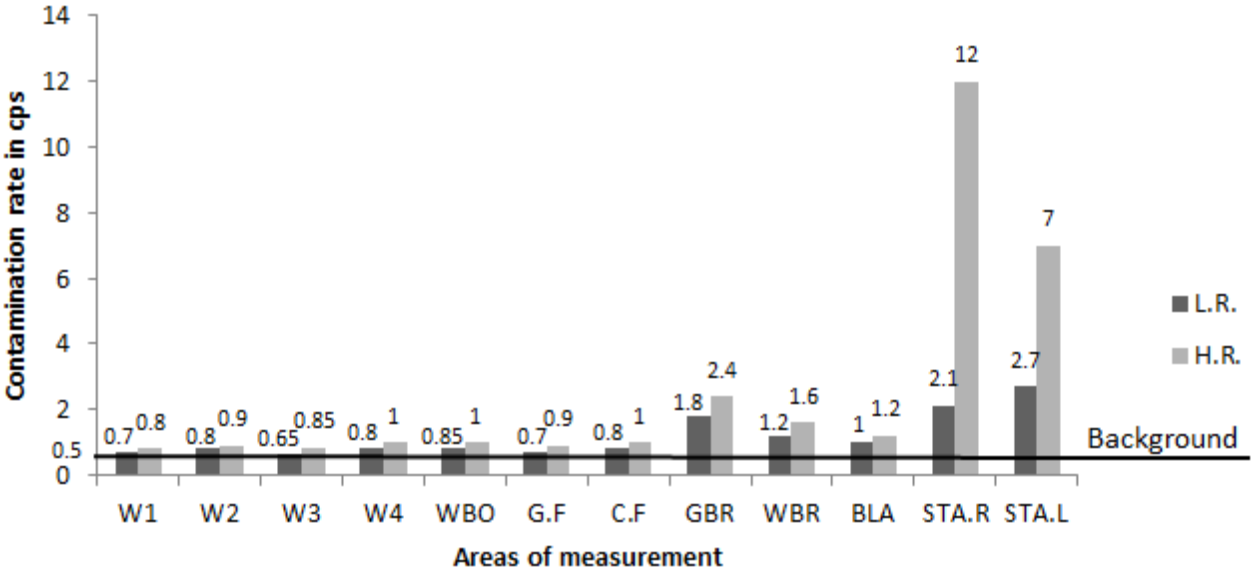

Figure (5) contamination rate in floor 9 before processes decontamination

Exposure rate measurements were performed before the decontamination processes. Figures (6, 7, 8, 9 and 10) show that.

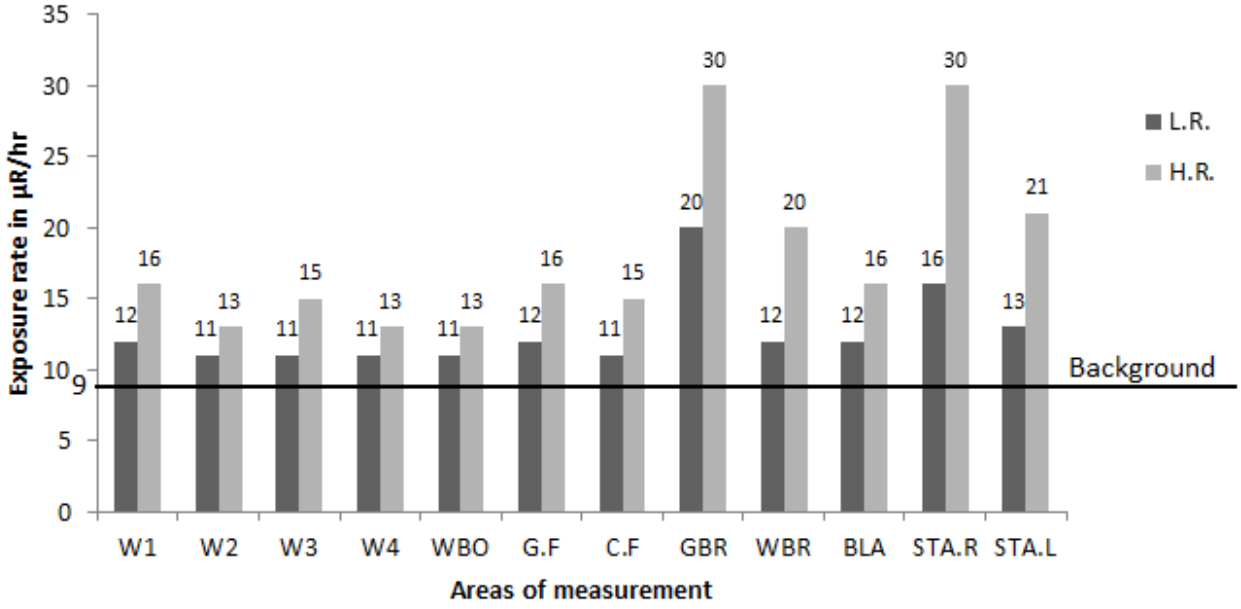

Figure (6) Exposure rate in floor 5 before the decontamination processes.

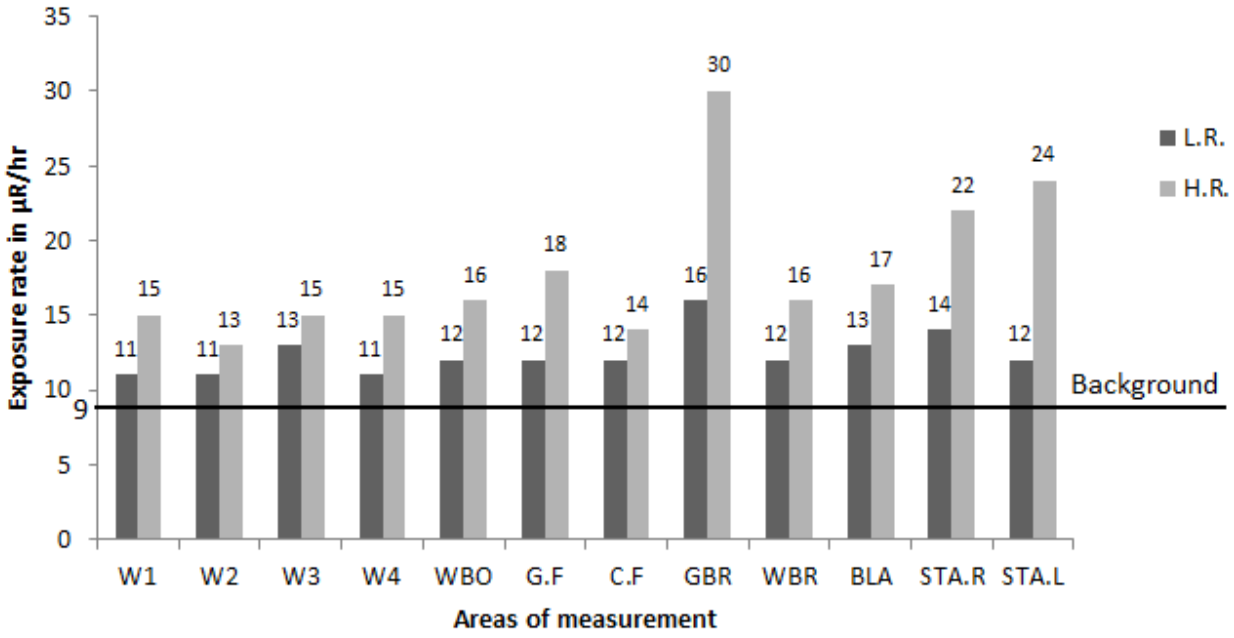

Figure (7) Exposure rate in floor 6 before the decontamination processes

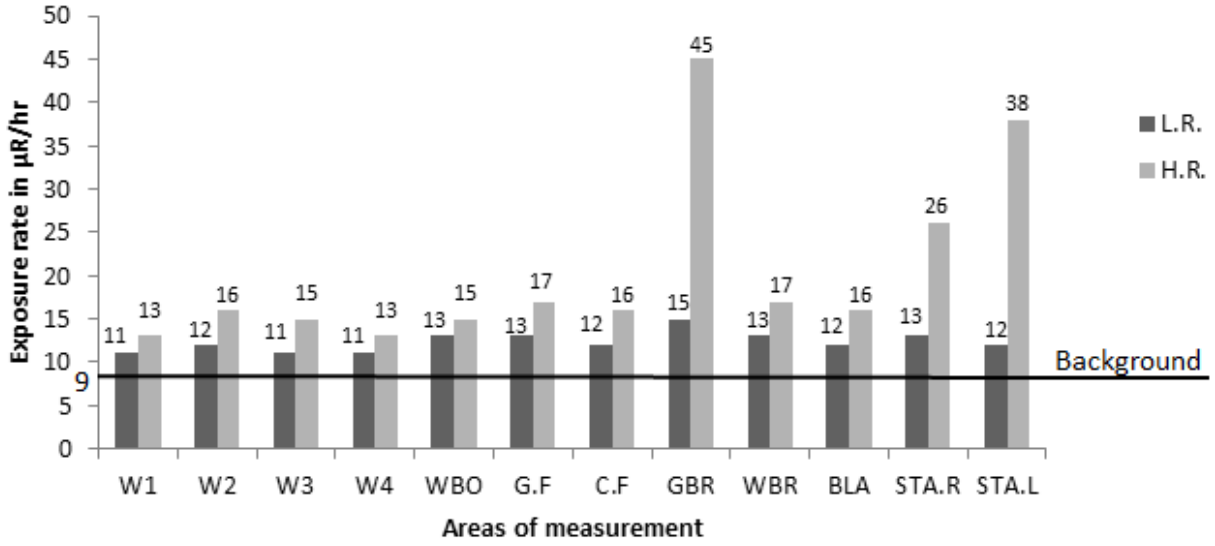

Figure (8) Exposure rate in floor 7 before the decontamination processes

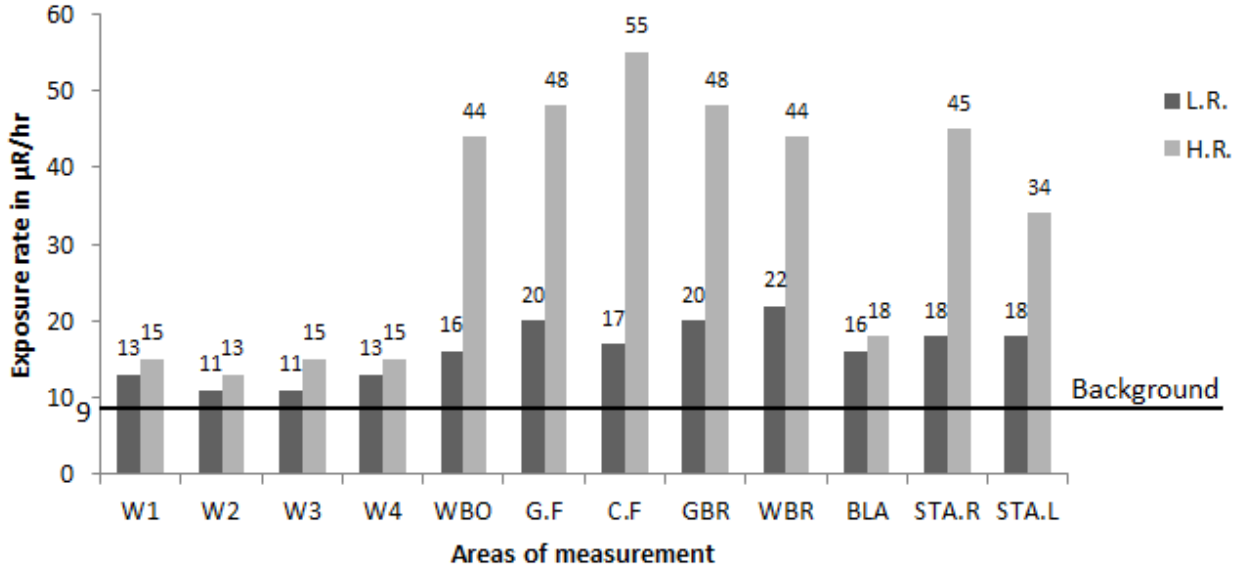

Figure (9) Exposure rate in floor 8 before the decontamination processes

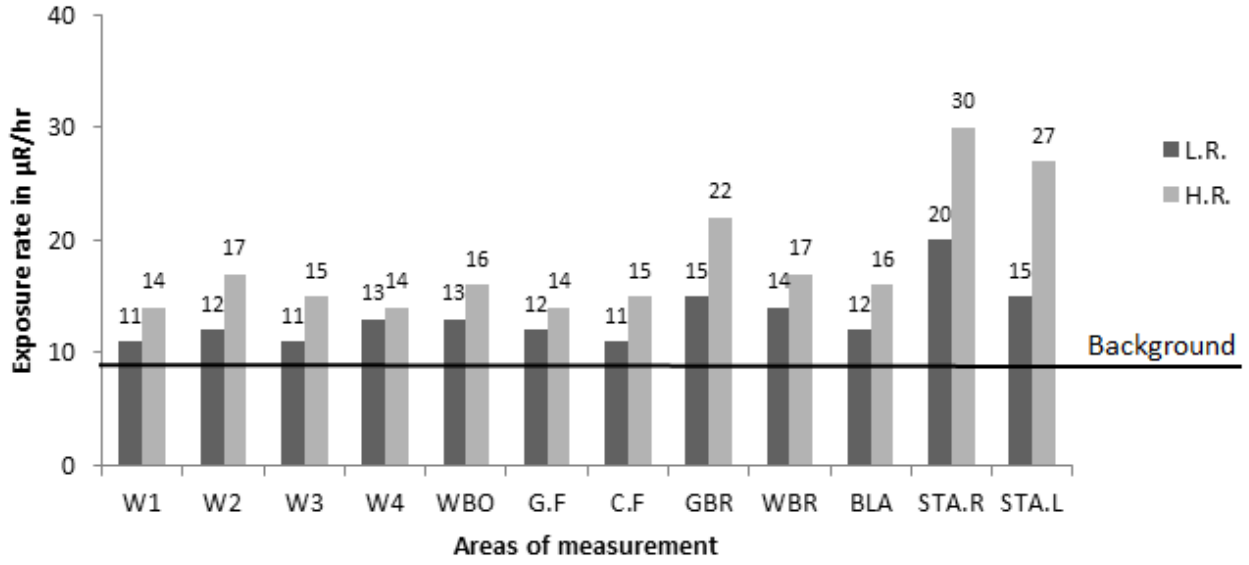

Figure (10) Exposure rate in floor 9 before the decontamination processes

Figures (11, 12) show the results of radiological survey in all floors which indicates the higher doses and contamination rates in eighth floor because the floor exposed to direct hits by depleted uranium bullets. The above figures indicate there were no significant levels of radioactivity detected in walls, and the spread of contamination in the bathrooms because the eighth floor was exposed to direct hit by depleted uranium bullets in the wall of bathroom from right side and that made a hole and contaminated large areas in floor in addition to contamination in internal walls of bathroom,

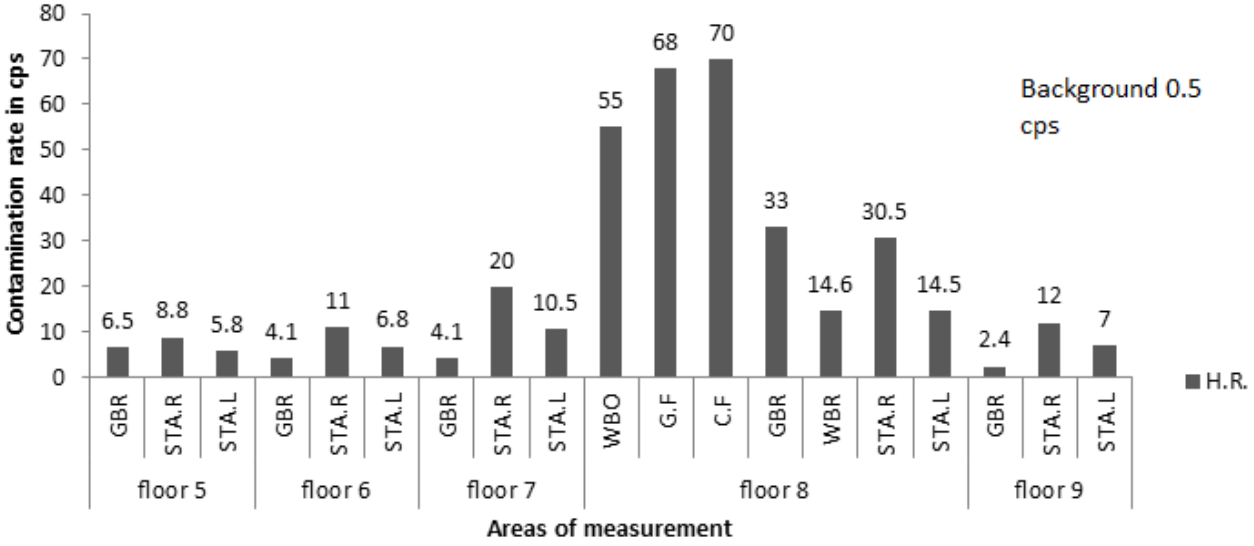

Figure (11) high value for contamination rate in all floors

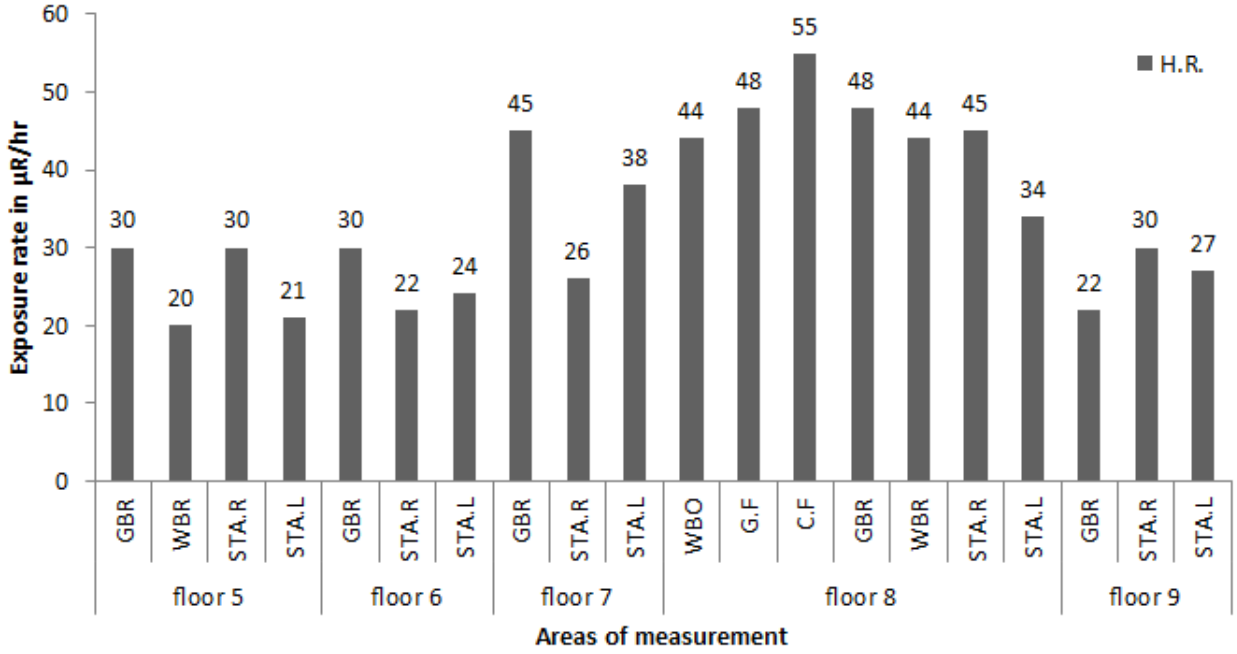

Figure (12) high value for exposure rate in all floors

The figures indicate the large spread of contamination in the bathrooms and stairs because some materials have been transported from the building to other areas without taking any environmental consideration, in addition to the building subject to movement of the winds. Therefore, the work has been focused on decontamination processes and lifted the contaminated soil which is considered more than two times higher than the natural levels when were using the portable radiation detection equipments, and sometimes were used mechanical decontamination techniques involved the removal of some thickness of the material of construction of walls, and the pipes waters especially in the eighth floor. The contaminated soil and waste collected in a special barrels intended for this purpose.

After the decontamination processes, soil samples were taken according to IAEA.The laboratory results indicated the presence of high concentrations of Th-234,and Pa-234m (an indicated nuclides for the presence of Uranium) of the soil samples in the floors (7 th,8 th and 9 th) therefore we repeated the decontamination processes by putting detector (CAB) on distance 0.5 cm and with speed less than 10cm/sec on the soils in the floors [6] .Than the contaminated soil Collected in a special barrels intended for this purpose .Soil samples were taken and the results are shown in figures (13,14).

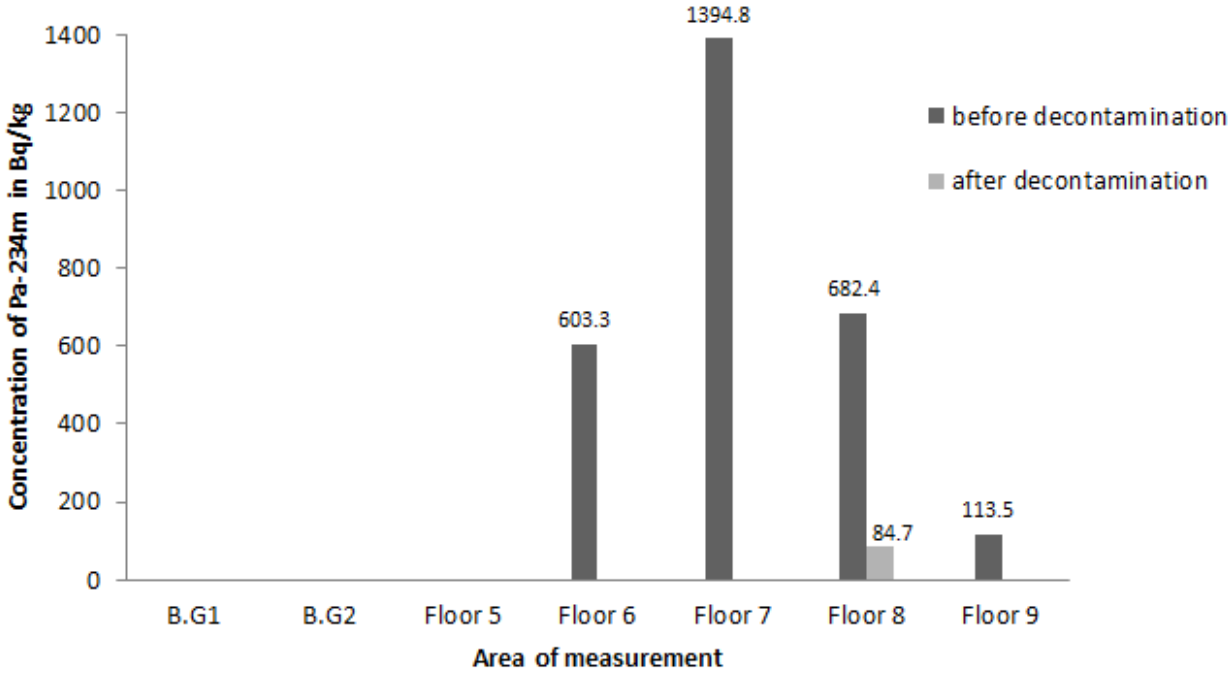

Figure (13) concentration of Pa-234m in soil sample before and after decontamination processes

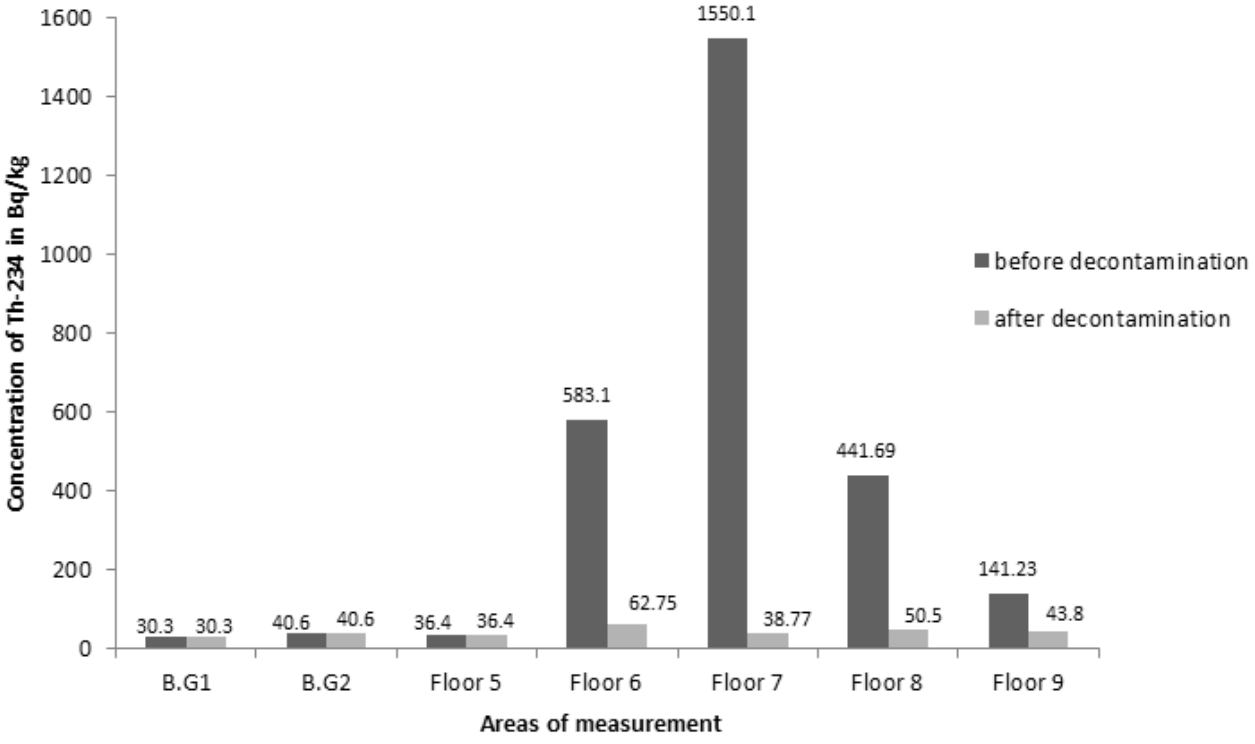

Figure (14) concentration of Th-234 in soil sample before and after decontamination processes

This laboratory results can be consider normal and slightly higher in comparison with natural background level, and these concentrations of the radioactive isotopes can be considered within the regulations limits of the environment.

CONCLUSION AND RECOMMENDATION

From field measurements, lab tests, and all other gathered information, the following be conclusions were drawn:

1- There is an increase in the radioactivity in the Tahreer Tower Building especially in the 8th floor because this floor was exposed to direct hit by depleted uranium bullets, and therefore most of the bathrooms in the floors are contaminated

2- Spreading of contamination in the building may be because many of materials have been transported from the building to other areas without taking any environmental consideration, in addition to the building subject to movement of the winds.

3- The exposure and contamination rates especially near the contaminated regions are higher than the background level and within a range between (11-55) µR/h and (0.55-70) c/s respectively while the background level varies between (10-8) µR/h and (0.4-0.6) c/s

4- Samples of contaminated soil which were taken from floors indicated higher Pa-234m content, which ranged between (113 .5-1394.8)Bq/kg while in the natural background of this isotope is nil.

Recommendations

1- The Iraqi Ministry of sciences and Technology must be receive support from the international community to increase expertise of the staff on technical level in methods of measuring and detection of DU.

2- The radiological survey must be doing in all metal scrap yards that have received scraps for the potential presence of DU.

3- Education and awareness-raising efforts on DU-related issues should be scaled up throughout the country to avoid that the population be accidentally exposed to DU.

4- The international community must work together to promote a decision prevent using DU weapons.

Symbols:

L.R.: Lower Reading
H.R.: Higher Reading
WBO: wall of bathroom from outside.
G.F: Ground of floor.

C.F: ceiling of floor.
GBR: ground of bathroom on the right side.
WBR: walls of bathroom on the right side.
BLA: bathroom on the left side including ground and walls.
STA.R: stairs on the right side.
STA.L: stairs on the left side.

References

1. U.S. Department of Defense: Environmental Exposure Report: Depleted Uranium in the Gulf War. Office of the Special Assistant for Gulf War Illness. U.S. Department of Defense. July 1-31 1998, p. 157. (1999).
2. U.S. AEPI: Health and environmental consequences of depleted uranium use by the U.S. Army. Technical report, June 1995. Army Environmental Policy Institute. Champaign, Illinois. (1994).
3. Jamal G. (1999) Gulf War Syndrome – a model for the complexity of biological and environmental interaction with human health. Adverse Drug React. Toxicol. Rev. 17 (1):1-17.
4. Ramsey C. (1996) Ban Depleted Uranium weapons" Metal of Dishonor, International Action Center, New York.
5. Eisenbid, M. (1987) Environmental radioactivity. 3rd Ed; Academic press Inc.
6. IAEA. (1998) characterization of radioactivity contaminated sites for remediation purpose, IAEA-TECDOC-1017, IAEA, Vienna.
7. IAEA. (1989) Measurement of Radionuclides in Food and the Environment, Technical Report Series 295, IAEA, Vienna.

Multi-User I Intrference Mitigation in TR UWB Receiver via Mid-point Impulse Correlation Technique

Dr. Natiq Abdullah Ali
Assist.Prof. in the Technical College of Management/ Baghdad
Foundation of Technical Education

E-mail :apdr_natiq@yahoo.com
Ph. 00964 7811332431

Abstract
Impulse radio-ultra wideband (IR-UWB) is a wireless technology system that offers a high data rate within a short range. Therefore, IR-UWB system is regarded as an excellent physical layer solution to the multi-piconet Wireless Personal Area Network (WPAN) applications. In spite of all the advantages of IR-UWB, there are several fundamental and practical challenges that need to be carefully addressed. The big and most important one among these challenges is the interference. In this paper, to largely suppress the Multi-User Interference (MUI), a very simple novel Midpoint Impulse Correlation (MIC) technique is proposed instead of the conventional correlation. The proposed technique is programmed using Matlab R2008b software and tested in various suggested scenarios close to the realistic multi-piconet WPAN environments using the dense multipath indoor IEEE 802.15.3a CM2. The performance results for the proposed technique exhibited lower SERs values as compared with the conventional correlation.

Keywords **: IR-UWB, MIC, IEEE 802.15.3a CM2, WPAN and SD .**

الخلاصة
أن ارسال النبضات الضيقة جدا Impulse Radio (IR)وبحزمة اتساع عريضة جدا Ultra-Wideband (UWB)هو نظام تكنولوجي لاسلكي يَعْرضُ سعة عالية ضمن مدى قصير. لذا، يُعتَبرُ نظام IR-UWB حَلاً ممتازاً للطبقةِ الفيزياوية لتطبيقاتِ شبكات الـ WPAN المتكونة من شبكات متعددة صغيرة جدا Multi-piconets . بالرغم مِنْ كُلّ فوائد نظام IR-UWB ، هناك عِدّة تحديات أساسية وعملية والتي مِن الضَّرُوري أَنْ تعامل بعناية كبيرة. أهم وأكبر تحدي والأكثر أهميةً بين هذه التحديات هو التداخلُ بأنواعه.ولغرض تَحسين أداءِ الانظمةِ في البيئاتِ متعددة المستخدمين، تم ابتكار واقتراح طريقة إرتباط بسيطة جداً بدلاً مِنْ الإرتباطِ التقليدي وهي إرتباط الاندفاع المنتصف Midpoint Impulse Correlation (MIC) وذلك لاخماد الـ MUI بشكل كبير جدا. الطريقة الجديدة المقترحة تم برمجتها باستخدام الـ Matlab R2008a وتم تجريبها في سيناريوهات مختلفة قريبة من بيئات شبكات الـ Multi-piconet WPANs الواقعية، وباستخدام القناة الداخلية الكثيفة متعددة الطرق نوع CM2IEEE 802.15.3a. إضافةً إلى ذلك، تم مقارنة الطريقة المقترحة بالطريقة التقليدية وأبدت قيم منخفضة للـ SERمُقارنة بها.

1. Introduction

As wireless communication systems are making the transition from wireless telephony to interactive internet data and multimedia types of applications, the desire for higher data rate transmission is increasing tremendously. As more and more devices go wireless, future technologies will face spectral crowding and coexistence of wireless devices will be a major issue. Ultra Wideband (UWB) offers attractive solutions for many wireless communication areas, including Wireless Personal Area Networks (WPANs), wireless telemedicine, and UWB wireless mouse, keyboard, and speakers [1]. With its wide bandwidth, UWB has the potential to offer much higher capacity than the current narrowband systems. From Shannon's formula for the capacity C in b/s in Additive White Gaussian Noise (AWGN), the capacity of the UWB system occupying bandwidth BW, as a function of the Signal to Noise Ratio (SNR) at a distance d between the transmitter and receiver is given by previous study [2]:

$$C(d) = BW \quad \log_2(1 + SNR(d)) \quad \text{..... (1)}$$

The function SNR (d) represents the effect of path losses on the transmitted signal. It can be seen that UWB systems offer their greatest promise for very high data rates for high BW.

The UWB system was often referred to as base-band, carrier-free or short impulse. A UWB signal is any signal whose fractional bandwidth BW_f is greater than 0.2 or occupies 500 MHz or more of the spectrum. The BW_f is given by previous study [2]:

$$BW_f = \frac{BW}{f_c} = 2\frac{(f_H - f_L)}{(f_H + f_L)} \quad \text{..... (2)}$$

Where f_H and f_L are defined as the highest and lowest frequencies, respectively in the transmission band and f_c is the center frequency.

UWB systems cover a large spectrum and interfere with existing users and narrow band services [3]. In order to keep this interference to the minimum, a spectral mask was specified for different applications which show the allowed power output for specific frequencies.

A possible technique for implementing UWB is the Impulse Radio (IR), which is based on transmitting extremely short (in the order of nanoseconds) and low power pulses [2]. These very short pulses in transmission result in a UWB spectrum [4]. Rather than sending a single pulse per symbol, a number of pulses determined by the processing gain of the system are transmitted per symbol.

The most popular approach for realizing UWB communications is Time Hopping(TH-IR). It allows a very simple transmitter structure that consists of only a baseband pulse generator, completely obviating the need for passband components like mixers, local oscillators, etc. However, the implementation of the receiver can be considerably more complex in a multipath environment.

2. The IEEE 802.15.3a Channel Standard Model

The IEEE 802.15.3a task group has evaluated a number of popular indoor Channel Models (CMs) to determine which model best fits the important characteristics from realistic channel measurements using UWB waveforms. The goal of the channel model is to capture the multipath characteristics of typical environments where IEEE 802.15.3a devices are expected to operate. Although many good models were contributed to the group, the model finally adopted was based on a modified Saleh-Valenzuela (S-V) model that seemed to best fit the channel measurements [5].

The multipath model adopted by the IEEE 802.15.3a committee for the evaluation of UWB physical layer proposals consists of the following discrete time impulse response [6]:

$$h(t) = X\sum_{k=0}^{K}\sum_{m=0}^{M}\alpha_{m,k}\delta(t - T_k - \tau_{m,k}) \quad \text{..... (3)}$$

where K is the number of clusters, M is the number of paths in the k^{th} cluster, $\alpha_{m,k}$ is the multipath gain coefficient, T_k is the delay of the k^{th} cluster, $\tau_{m,k}$ is the delay of the m^{th} MPC (ray) relative to the k^{th} cluster arrival time T_k, and {X} represents the log-normal shadowing. Furthermore, h(t) can also be written as [7]:

$$h(t) = \sum_{l=1}^{L}\alpha_l\delta(t - lT_m) \quad \text{..... (4)}$$

where α_l is the multipath gain coefficient, represents the sum of all MPCs arrived in l^{th} time bin and L is the number of resolvable MPCs. Assuming that T_m is equal to the IR-UWB chip interval T_c, then h(t) becomes:

$$h(t) = \sum_{l=1}^{L}\alpha_l\delta(t - lT_c) \quad \text{..... (5)}$$

and by letting $\tau_l = lT_c$, then h(t) becomes:

$$h(t) = \sum_{l=1}^{L}\alpha_l\delta(t - \tau_l) \quad \text{..... (6)}$$

3. IR-UWB Receiver Options

High capacity, high-data rate, simple, power-efficient, low-cost, and small IR-UWB receivers design is a challenging task [1].

A generic UWB receiver structure is shown in Fig. (1) [1,6]. The optimal matched filtering implemented as Rake with a simple single correlator receivers correlate the received signal with a local template. The local template can be a pulse template, a frame template, or a template that includes multiple pulses to include the relative delays between pulses based on the TH code. In either case, the template needs to be

estimated locally based on the received signal by transmitting some training sequences. This type of receiver, which correlates the received signal with a template, is often referred to as "locally generated reference" systems or simply as "correlation" receivers (switch at point 2). Alternatively, the received signal can be correlated by itself, which leads to "autocorrelation" receiver structures (switch at point 1) i.e., the TR receiver.

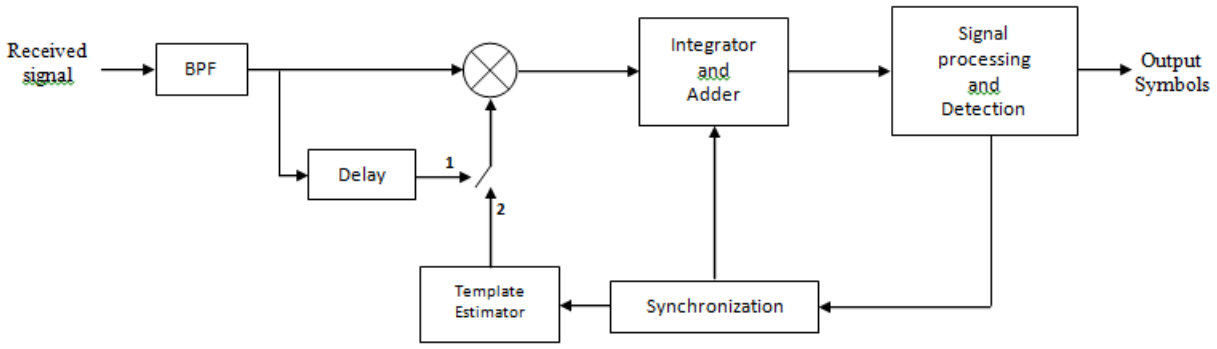

Fig. (1): A Generic IR-UWB receiver structure

4. IR-UWB TR-Based Scheme

One of the key challenges for IR-UWB system is the construction of low-cost receivers that work well in multipath environments. From the previous section, it's known that the coherent Rake receiver offers optimal performance, relying on enough fingers to accurately capture all or a significant part of resolvable MPCs.

However, a large discrepancy in performance exists between the implementations and the theoretically optimal receivers. In IR-UWB system, the number of resolvable paths could reach tens to over a hundred in typical indoor propagation environments, which imposes technical hurdles as well as implementation difficulties. In order to capture a considerable portion of the signal energy scattered in MPCs, a conventional Rake requires an impractically large number of Rake fingers. In addition, Rake reception performance requires accurate channel and timing knowledge, which is quite challenging to obtain as the number of resolvable paths grows. The received pulse shapes of resolvable multipath are distorted differently due to diffraction, which makes it suboptimal, and one must use line-of-sight signal waveform as the correlation template in Rake reception which is impossible at all. Because of these issues unique to IR-UWB systems, an optimal Rake receiver design becomes either ineffective or very complicated [8].

The basic principle in TR-based schemes is to transmit a reference (unmodulated) pulse along with the data (modulated) pulse. The reference pulses and the data pulses are transmitted with a delay T_d between them. When the delay is less than the T_{mds}, the reference and data pulses can be assumed to be affected similarly due to the channel. Therefore, instead of using a local template, the TR scheme uses the reference pulses as the template for correlating the data pulses,

and for the demodulation of the transmitted information. TR transceiver structure is shown by the block diagram in Fig. (2) [1,9].

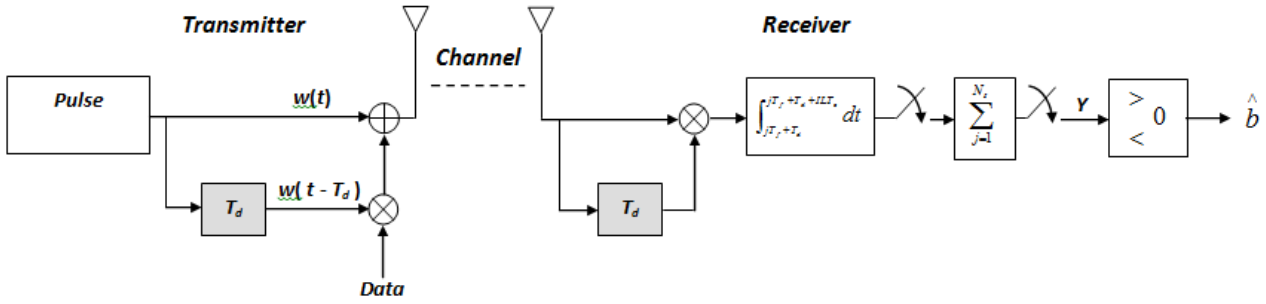

Fig. (2): Block diagram of a simple IR-UWB TR transceiver system

Another important issue in TR scheme is the use of the noisy templates for the correlation. In other words, as the TR scheme makes use of a "dirty" reference to detect the data, it still suffers from a larger performance degradation compared to a matched filter scheme [10].

In addition to single user performance, multiple accessing capabilities of TR schemes and techniques to improve multiuser performance are also important. If not designed properly, TR schemes are expected to be more susceptible to MUI and to other interference sources. First of all, the TR schemes experience more interference due to the integration of the multiplier output over a window that both desired pulses and possible interfering sources exist.

However, IR-UWB TR also has some disadvantages. It is often considered as a low data rate scheme because of implicit assumptions that the pulse spacing T_d in a doublet should be longer than the T_{mds} to prevent IPI, and the T_f should be chosen such that there is no IFI: together this leads to $T_f > 2T_{mds}$. Since both pulses in a doublet go through the same noisy channel, the correlating operation enhances the noise, which degrades the BER performance. In most IR-UWB TR schemes, signals are integrated over the full frame or symbol period, which may accumulate noise, especially at the end of the frame (or the tail of the multipath channel) where the signal strength is much weaker or even absent [11].

A conventional TR signaling carries bit information using the phase difference between the reference and data pulses occurring with fixed relative delay in a frame. The i^{th} bit's transmitted signal of conventional TR using BPSK modulation can be written as [12]:

$$S_{tx}^{(v)}(t) = \sqrt{\frac{E_f^{(v)}}{2}} \sum_{j=iN_s}^{(i+1)N_s-1} [w_{tx}(t - jT_f - c_j^{(v)} - \tau_o^{(v)}) + b_i^{(v)} w_{tx}(t - jT_f - c_j^{(v)} - T_d^{(v)} - \tau_o^{(v)})] \quad \text{..... (7)}$$

Where $w_{tx}(t)$ is the unit-energy transmitted pulse of duration T_p (also equal to T_c). T_f is the frame time to transmit a pair of reference and data pulses, and E_f here is defined as the frame energy. To avoid the IFI, it is assumed that $T_f \geq T_h + T_d + T_{mds}$, where T_d is the relative time delay between the reference and data pulses, and is assumed to be an integer multiple of chip time ($T_d = \Delta T_c$), where

Δ is an integer. b_i is the i^{th} binary bit, taking on the values of {−1, +1} with equal probabilities. Note that, to allow for multiple access a user specific THS is employed to randomize the location of the pulse pair in each frame. The received signal r(t) is given by:

$$r(t) = \sum_{v=1}^{N_u} h^{(v)}(t) \otimes S_{tx}^{(v)}(t) + n(t) \quad \text{..... (8)}$$

Assuming perfect synchronization, the sum of all correlated values over N_s frames is used as the decision statistic to detect the i^{th} transmitted data symbol for v^{th} user, the decision statistic ($Y_{bit}^{(v)}$) is given by:

$$Y_{bit}^{(v)} = \sum_{j=1}^{N_s} \int_{jT_f + c_j^{(v)} + T_d^{(v)}}^{jT_f + c_j^{(v)} + T_d^{(v)} + ILT_c} r(t - T_d^{(v)}) \, . \, r(t) \quad dt \quad \text{..... (9)}$$

5. Integration Length Optimization

The critical design parameter for IR-UWB TR receivers is the Integration Length (IL) [13].At the integrator block - Fig. (2) -, the integration was done for the entire length of the T_{mds}. But, since indoor wireless channels change with location and distance between transmitter and receiver, it was realized that T_{mds} and thus integration time should be jointly taken into account to optimize the performance of systems. For a TR system working in an environment for example CM2 having a T_{mds}, the IL determines the amount of pulse energy as well as the noise captured, thus affecting the effective SNR of the decision variable.

The IL is assumed to be an integer multiple of the chip time, denoted by ILT_c, satisfying $0 < IL\ T_c \leq T_{mds}$.

6. The proposed Midpoint Impulse Correlation Technique

In the previous receiver, the IPI is completely removed. The multiple access technique that used is the TH. In fact, this techniqueis essentially used to distinguish between access users, but they cannot be hardly removed, mitigated, or prevented of serious MUI. In other words, they are not appropriate for concurrent schemes. The question arises here, what happens if the interferer pulses are largely overlapped with the intended pulses in the overlapped or non-overlapped portionof the reference and data waveforms? Certainly, the correlation process between the reference and data waveforms will have large errors and so the decision process will overwhelm with errors that yield a strong SER degradation. The correlator will in this case make a correlation among the reference, data, and the huge interferer pulses along the entire channel access delay that contained the replicas of pulses due to multipath channel.

The results of the correlation process will be wrong because of the collided pulses. To deal with this problem, a novel correlation technique is proposed called Midpoint Impulse Correlation (MIC). Thus, instead of performing a complete correlation between one reference and one data pulse, a special correlation can be performed between only the middle impulses (samples) of the two waveforms. The middle sample has the larger amplitude and the probability it is affected with

collided pulses will be largely decreased. In doing this function, first the resulted total received reference and the delayed data waveforms, $R_{ref}(t)$ and $R_{data}(t)$ respectively are individually multiplied by a mask function $F_{mask}(t)$ which is defined as:

$$F_{mask}(t) = \sum_{k=1}^{IL} \delta(t - (k-1)T_c - T_p / 2) \quad \text{..... (10)}$$

The principle of the mask function is illustrated in Fig. (3) that shows the multiplication with pulse replicas due to multipath effect. In fact, the multiplication is done along the IL instead of T_{mds}, and therefore this is another simplification for the mask function.

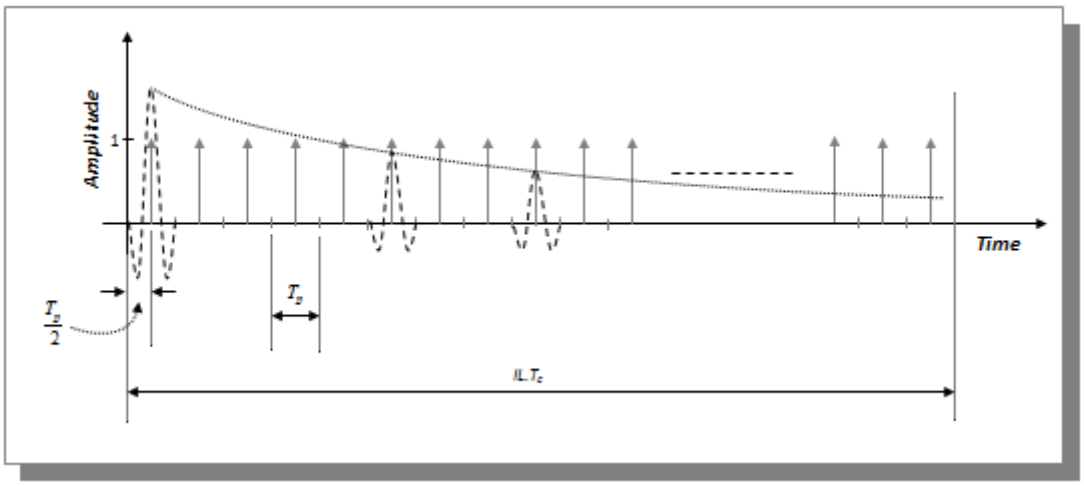

Fig. (3): The mask function

Anyway, the resulting sampled version of $R_{refe}(t)$ and $R_{data}(t)$ are then correlated to get the metric quantity. Certainly, a large portion of the signal energy will be lost due to the above process especially if there is no MUI.

7. System and Channel Models

The general block diagram of the IR-UWB indoor physical layer communication system investigated and programmed in this paper is shown in Fig. (4) with IEEE 802.15.3a indoor multipath channel and IR-UWB TR receiver.

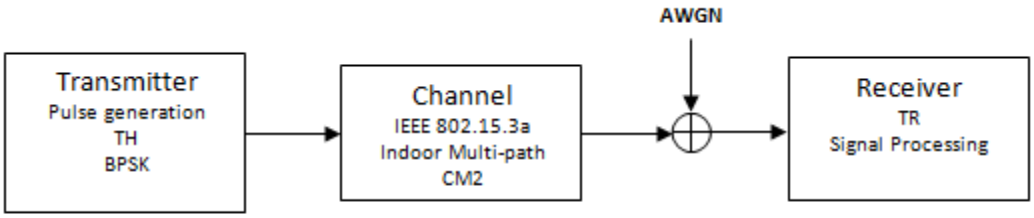

Figure (4): IR-UWB communication system used in this paper

Also, the MUI model that is used in this work is shown in Fig. (5).

The NLOS IEEE 802.15.3a indoor WPAN multipath CM2 has been used with an exponentially decaying delay profile. The CM2 is the best fit of the piconet dimension that does not exceed 4m which is the same work distance of CM2. For every new transmitted data symbol, a single CM2 channel realization is chosen among 10,000 bad and good already prepared channel realizations for each transmitted user's symbol for the desired and interferer piconets.

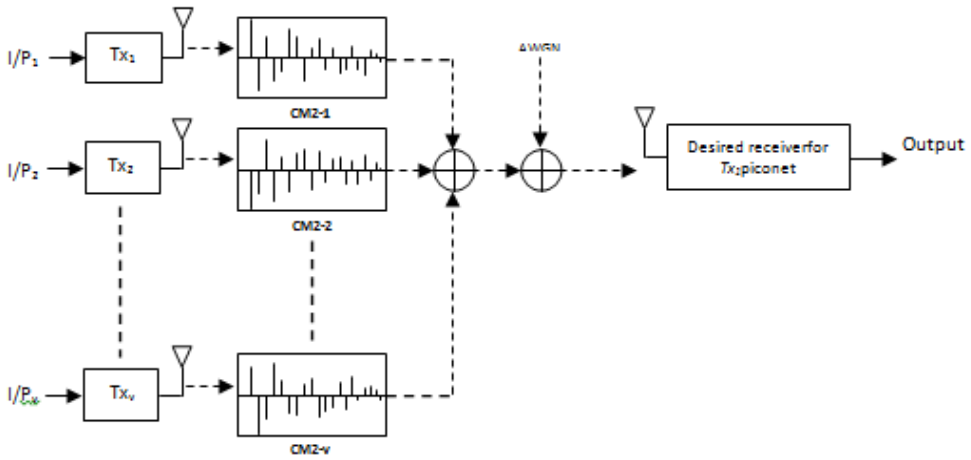

Fig. (5): The MUI model in the presence of multipath and AWGN channels

8. *Main System Parameters*

The system parameters are chosen to satisfy some of the assumptions listed in the previous sections. All parameters are fixed unless mentioned otherwise. Table (1) show the system parameters that will produce the results presented in section 9.

Table (1): Simulation parameters

Parameter	***Symbol***	***Value***
Sampling period	T_{sam}	0.02 ns
Pulse duration	T_p	0.4 ns
Chip time	T_c	0.5 ns
Pulse shaping factor	τ_{sf}	0.24 ns
Channel bin duration	T_m	0.5 ns
Channel duration	T_{mds}	70 bins
Path loss exponent [34]	n	3.5
Number of pulses per symbol	N_s	variable
Received Signal-to-Noise ratio	$(S/N)_{RX}$	variable
Desired transmitted power in [dBm/Hz][8]	$(PT_1)_{Tx}$	variable
Interferer transmitted power in [dBm/Hz][8]	$(PT_{int})_{Tx}$	variable
User 1 distance	d_1	variable
Interferers distances	d_{int}	variable
Piconet diameter	------	4 m
Users' delays	$\tau^{(v)}$	$(0\text{-}T_f)$ ns
TH length	$N_{h.}$	50 chips
WPAN dimension	------	(0 – 10) m
Pulse delay for SD receiver	------	1 bin
Frame duration	T_f	variable
Number of symbols generated by the source	------	40000 sym.

9. *Performances of the Proposed TR Receivers*

9.1 Determining of Optimum IL

The first step in performing the simulation is to determine the optimum IL value at different IL range between (1-100) channel bins. The choice of optimum IL is a very important step and will be used in the next performance steps.

In addition, d_1 and d_{int} are set to 3.16 m to maintain the integer $(S/N)_{Rx}$ ratios shown in Table (1) for various PT_1 corresponding values.

The performance is evaluated in terms of average SER for the four proposed besides the SD receivers using the sets of parameters shown in Table (2):

Table (2): Various sets of parameters to determine optimum IL.

Set	$(S/N)_{Rx}$ [dB]	$(PT_{int})_{Tx}$ [dBm/Hz]	N_s	N_u
1	0	----	4	1
2	14	-98	4	2
3	14	-98	4	3
4	14	-98	4	4

In addition, d_1 and d_{int} are set to 3.16 m to maintain the integer $(S/N)_{Rx}$ ratios shown in Table (2) for various PT_1 corresponding values.

The SER versus IL for set 1 parameter is plotted in Fig. (6). In this figure it can be concluded that optimum integration interval lies in the range of (20−40) bins and this has the best performance. As an important notice, the SD receiver has the best performance in single piconet case, hence it achieved about 6×10^{-4} SER. On the other hand, the SD/MIC receiver achieved the worst performance. This is due to the low S/N value that makes the decision devices in the two receivers in a challenge task to determine the estimated symbol. On the other hand, the receiver based on MIC has achieved very high SER values due to lose of energy during the special correlation process as compared with the conventional correlation.

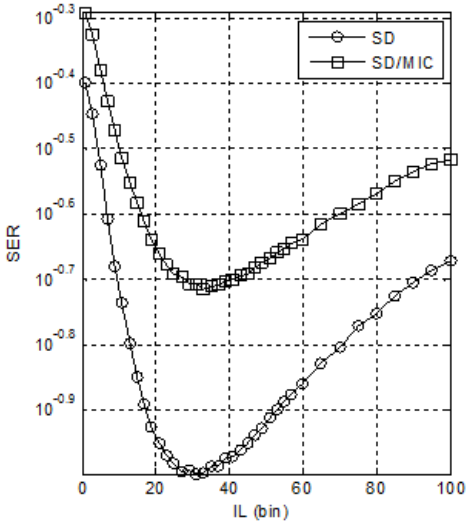

Fig . (6): The IL for set 1

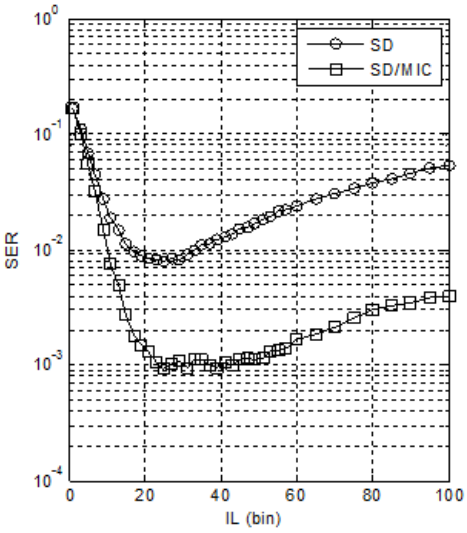

Fig . (7): The IL for set 2

In general, the performance suffers when enough energy is not captured before the integration interval. Also, the SER is increased beyond the integration interval due to the small amplitude gain of the channel (the channel tail) and therefore more noise will largely degrade the performance.

When N_u = 2,3 and 4, an inversion point is noticed in the SER performance of the SD/MIC receiver as shown in Figs. (7-9) for set 2 parameters. The optimal IL region is about (20-33) bins for the SD receiver, while it is about (22-37) bins for the SD/MIC receivers. In overall, the IL regions for all

receivers are decreased due to the MUI that makes the receivers depend on the first fewer channel paths in the beginning of the multipath channel that have large gains. The worst SER is obtained for the SD receiver due to the MUI that overwhelm the correlation process to yield wrong quantities.

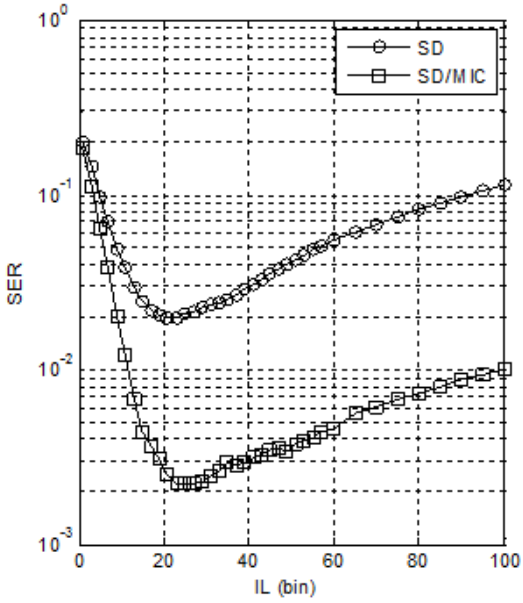

Fig. (8): The IL for set 3

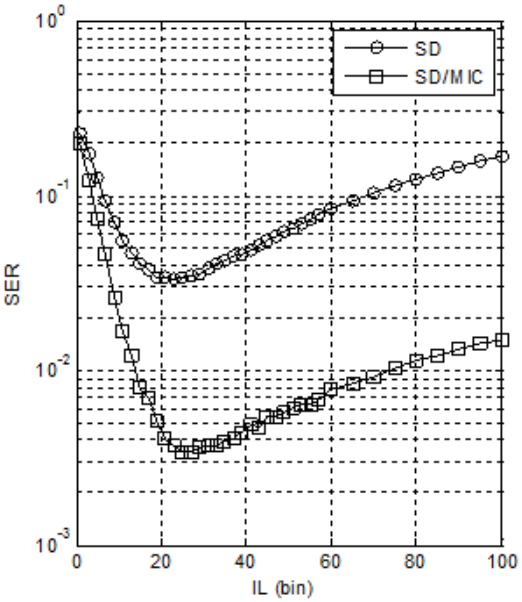

Fig. (9):The IL for set 4

Now, the ILs selected values is based on the minimum ones whatever the SER values which somehow reduces receiver complexity (shorter and fixed IL) without causing too much performance loss. This is because of the nature of the multi-piconets concurrent transmission. In other words, the expectation that only a single piconet is active in a multi-piconet WPAN is very weak. Therefore, IL = 22 bins is a good choice and may be chosen for SD receivers, whereas IL = 29 bins is also a good choice and may be chosen for the SD/MIC receiver as an optimum ones.

The choice of the optimal IL values is very important step for the next performance simulations as will be seen later.

9.2 Performance with Single-piconet w/o IFI and ISI

A simulation is done to study the performance of the proposed receivers as a function of the received S/N per frame at the receiver input for N_s = 4. Fig. (10) shows the performance without the effects of IFI and ISI for a single piconet (N_u=1). The T_g in this case is set 50 bins. Remember that inthese cases the channel response to the transmitted pulse is completely died out before the transmission of the next pulse. It's clear from the result of the simulation that the SD receiver outperforms the others. Hence, at 10^{-4} target SER, it needs about 2 dB of S/N.

The performance with the effects of hard IFI and soft ISI for the same single piconet (N_u = 1) is shown Fig. (11). The T_g is reduced to 25 bins. In this case each adjacent frame belongs to a certain symbol is overlapped resulting in hard IFI. Besides, the last frame for symbol (i) is overlapped with the first frame of symbol (i+1) resulting in the so called soft ISI. Certainly, the data rate is also increased due to the reduction in T_f. Anyway, it's interesting to notice that there are very low degradations in the achieved SER values for all receivers as compared with the case without IFI and ISI and these low degradations are hardly noticeable.

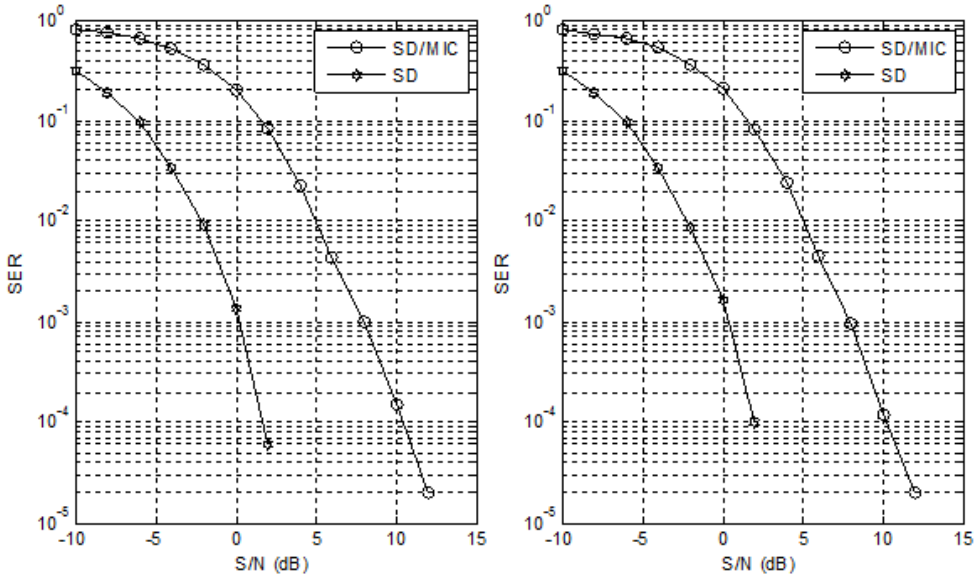

Fig. (10) Without IFI and ISIFig. (11) With IFI and

9.3 Performance with Multi-piconets w/o IFI and ISI.

In general, it is not difficult to see that increasing the number of interfere piconets ($N_u = 2$) can degrade the performance of all receivers as shown in Fig. (11) for the same value of N_s. This is Because of more MUI pulses which mean more collision pulses with the IR-UWB signal of the desired piconet.

The performance of the receivers without IFI and ISI is shown Fig. (12). It's very obvious that the SD/MIC receiver outperform the SD receiver due to the MIC technique which hardly mitigates the MUI.

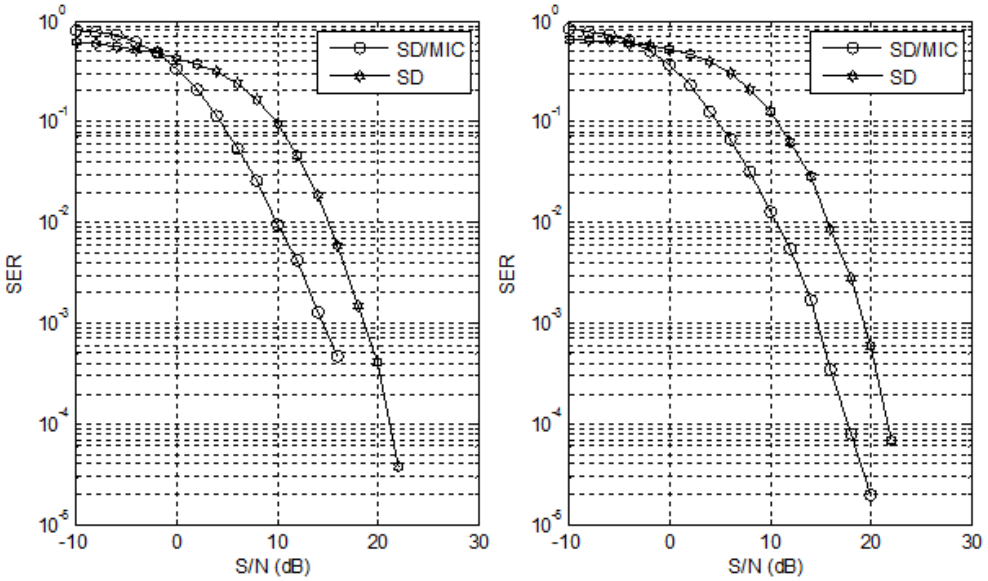

Fig. (12) Without IFI and ISIFig. (13) With IFI and

In another test, the two receivers were subjected to hard IFI and soft ISI. The performance was plotted and shown in Fig. (13) for two piconets ($N_u = 2$). The T_g was also reduced to 25 bins. It's clear that there were very low degradations in the achieved average SER for all receivers as

compared with the case without IFI and ISI and these degradations are noticed in the plot. It should be kept in mind that an increase in the information rate was obtained due to the reduction in T_f.

10 Conclusions

The objectives of this paper are to design, semi-analyze and investigate the performance of multi-piconet WPAN IR-UWB receivers. The performance was evaluated in the presence of MUI, ISI, IFI, IPI, indoor dense multipath IEEE 802.15.3a CM2, and AWGN. Also, a novel multiple access method and a very simple novel correlation technique will also proposed in this paper to mitigate the MUI in UWB TR receivers.It's shown also and concluded that the MIC technique is a very simple method to largely mitigate hard MUI and clearly it is a feasible solution for practical TR implementations.

References

1. Arslan, H., Chen, Z., Gabriella, M. (2006) Ultra Wideband Wireless Communication, John Wiley & Sons, Inc.,.
2. Saeed, R., Khatun, S., Ali, B. (2005) Ultra Wideband (UWB) Ad-Hoc Networks: Review and Trends. J Comput. Sci. 1: 35-39.
3. Nardis, L., Giancola, G., Benedetto, M. (2003) A Power-Efficient Routing Metric for UWB Wireless Mobile Networks", Proc. of Vehicular Technology Conference, Orlando, USA.
4. Oppermann, I., Hamalainen M., Iinatti, J. (2004) UWB Theory and Applications, John Wiley & Sons Ltd.
5. Gubner, J., Hao, K. (2005) Analysis of the IEEE 802.15.3a UWB Channel Model, IEEE Journal on Selected Areas in Communications.
6. Durisi, G., Benedetto, S. (2005) Comparison between Coherent and Noncoherent Receivers for UWB Communications, EURASIP Journal on Applied Signal Processing (3):359–368.
7. Glisic, S. (2006) Advanced Wireless Networks 4G Technologies, John Wiley & Sons Ltd.
8. Qiu, R., Liu, H., Shen, X. (2005) Ultra-Wideband for Multiple Access Communications, IEEE Communications Magazine.
9. Dang, H., Veen, A. (2007) Signal Processing for Transmit-Reference UWB, Proceedings of SPS-DARTS 2007, 3rd Annual IEEE BENELUX/DSP Valley Signal Processing Symposium: 55-61.
10. Guo, N., Qiu, R. (2006) Improved Autocorrelation Demodulation Receivers Based on Multiple-Symbol Detection for UWB Communications, IEEE Transactions on Wireless Communications. 5(8).
11. Dang, Q., Veen, A. (2007) Signal Processing Model and Receiver Algorithms for a Higher Rate Multi-User TR-UWB System', Proc. IEEE ICASSP, Honolulu: III-(581-584).
12. Kim, D., Jia, T. (2008) M-Ary Orthogonal Coded/Balanced Ultra-Wideband Transmitted-Reference Systems in Multipath, IEEE Transactions on Communications. 56(1).
13. Franz, S., Mitra, U. (2004) Integration Interval Optimization and Performance Analysis for UWB Transmitted Reference Systems", Proc. UWBST, Pages (26-30), Kyoto, Japan.